

Monte Carlo simulation of $O(2)$ ϕ^4 field theory in three dimensions

Peter Arnold

Department of Physics, University of Virginia, P.O. Box 400714, Charlottesville, VA 22904-4714

Guy Moore

Department of Physics, University of Washington, Seattle, Washington 98195-1560

(December 2, 2024)

Abstract

Using standard numerical Monte Carlo lattice methods, we study non-universal properties of the phase transition of three-dimensional ϕ^4 theory of a 2-component real field $\phi = (\phi_1, \phi_2)$ with $O(2)$ symmetry. Specifically, we extract the renormalized values of $\langle \phi^2 \rangle / u$ and r/u^2 at the phase transition, where the continuum action of the theory is $\int d^3x [\frac{1}{2} |\nabla \phi|^2 + \frac{1}{2} r \phi^2 + \frac{u}{4!} \phi^4]$. These values have applications to calculating the phase transition temperature of dilute or weakly-interacting Bose gases (both relativistic and non-relativistic). In passing, we also provide perturbative calculations of various $O(a)$ lattice-spacing errors in three-dimensional $O(N)$ scalar field theory, where a is the lattice spacing.

I. INTRODUCTION

A long standing problem is how to compute the first correction ΔT_c , due to interactions, to the critical temperature T_c for Bose-Einstein condensation of a very dilute non-relativistic homogeneous Bose gas in three dimensions. In Ref. [1], we review how this problem is related to three-dimensional $O(2)$ ϕ^4 field theory [2], present the results of lattice simulations of that theory, and so determine ΔT_c . The purpose of the present work is to provide details of those simulations. The lattice results presented here can also be applied to relativistic Bose gases [3,5] and to non-relativistic gases in a trapping potential [5].

Three-dimensional $O(2)$ ϕ^4 theory has the continuum action

$$S = \int d^3x \left[\frac{1}{2} |\nabla \phi|^2 + \frac{1}{2} r \phi^2 + \frac{u}{4!} (\phi^2)^2 \right], \quad (1.1)$$

where $\phi = (\phi_1, \phi_2)$ is a two-component real field and $\phi^2 \equiv \phi_1^2 + \phi_2^2$. For fixed u , we will vary r to reach the second-order critical point $r_c(u)$ of this model. The shift in the critical

temperature of a non-relativistic homogeneous single-species Bose gas is given in terms of this theory by [2]

$$\frac{\Delta T_c}{T_0} = -\frac{2mk_B T_0}{3\hbar^2 n} \Delta \langle \phi^2 \rangle_c, \quad (1.2)$$

where m is the boson mass, n is the number density, and

$$\Delta \langle \phi^2 \rangle_c \equiv [\langle \phi^2 \rangle_c]_u - [\langle \phi^2 \rangle_c]_0 \quad (1.3)$$

represents the difference between the critical-point value of $\langle \phi^2 \rangle$ for the cases of (i) u non-zero and (ii) the ideal gas $u=0$ (with $r \rightarrow 0$ from above). The result for $\Delta \langle \phi^2 \rangle_c$ in the O(2) theory (1.1) can only depend on u and so, by dimensional analysis, it must be proportional to u . A primary goal will be to discuss in detail the measurement of the numerical constant $\Delta \langle \phi^2 \rangle_c / u$ from lattice Monte Carlo simulations of the theory. As reported in Ref. [1], our result is

$$\frac{\Delta \langle \phi^2 \rangle_c}{u} = -0.001195 \pm 0.000017. \quad (1.4)$$

The critical value r_c of r is also useful for various theoretical applications, such as determining corrections to the value of the chemical potential at the transition [5], or to the critical temperature of a trapped gas [5], or to the critical temperature of ultrarelativistic ϕ^4 theory at zero chemical potential [4]. The ϕ^2 interaction is associated with an ultraviolet (UV) divergence of the three-dimensional theory and so must be renormalized. If one chooses the renormalization scale $\bar{\mu}$ to be of order u then, by dimensional analysis, the renormalized value of $r_c(\bar{\mu})$ must be proportional to u^2 . The precise scheme used to renormalize r , and the precise choice of $\bar{\mu}$, is a matter of convention. In this paper, we will report a measurement of the numerical constant r_c/u^2 for r defined by dimensional regularization and modified minimal subtraction ($\overline{\text{MS}}$) at a renormalization scale of $\bar{\mu} = u/3$. Our result is

$$\frac{r_c^{\overline{\text{MS}}}(u/3)}{u^2} = 0.0019192 \pm 0.0000020. \quad (1.5)$$

One can convert to other choices of $\bar{\mu}$ by the (exact) identity

$$\frac{r_c^{\overline{\text{MS}}}(\bar{\mu}_1)}{u^2} = \frac{r_c^{\overline{\text{MS}}}(\bar{\mu}_2)}{u^2} + \frac{2}{9(4\pi)^2} \ln \frac{\bar{\mu}_1}{\bar{\mu}_2}. \quad (1.6)$$

In section II, we discuss the lattice action we use, its relationship to continuum fields and parameters, how we correct for $O(a)$ lattice spacing errors, and the algorithms we use for simulation. Section III details our procedure for finding the transition, based on the method of Binder cumulants. In section IV, we present our initial data, show that we have simulated moderately large volumes, and then discuss how to analyze the remaining finite-volume corrections by making use of the known critical exponents associated with this universality class. The corresponding numerical extrapolations of the finite-volume corrections are given in section V. Numerical extrapolation of the continuum limit is presented in section VI. A table of all our raw data for various size lattices and values of coupling may be found in

Appendix A. The derivations of the $O(a)$ lattice-spacing corrections used in this paper are given in Appendix B. The remaining appendices include various discussions of scaling laws used in the text, an analytic calculation of results for small lattice volumes, and a critical discussion of one of the early simulations, in the literature, of the Bose-Einstein condensation temperature of dilute non-relativistic gases.

II. LATTICE ACTION, MEASUREMENT, AND ALGORITHM

The bare lattice Lagrangian has the form

$$\mathcal{L} = a^3 \sum_{\mathbf{x}} \left[\frac{1}{2} (-\Phi_1 \nabla_{\text{lat}}^2 \Phi_1 - \Phi_2 \nabla_{\text{lat}}^2 \Phi_2) + \frac{r_0}{2} (\Phi_1^2 + \Phi_2^2) + \frac{u_0}{4!} (\Phi_1^2 + \Phi_2^2)^2 \right], \quad (2.1)$$

where a is the lattice spacing. In an actual simulation, one invariably chooses lattice units where $a=1$, or equivalently works with rescaled fields and parameters $\Phi^L = a^{1/2}\Phi$, $r_0^L = a^2 r_0$, and $u_0^L = a u_0$. For the sake of presentation, however, we will generally avoid specializing to lattice units.

We work on a simple cubic lattice, and will work in cubic volumes $L \times L \times L$ with periodic boundary conditions, corresponding to $(L/a)^3$ sites. The simplest possible implementation of the lattice Laplacian, which we call the “unimproved” choice ∇_{U}^2 , would be

$$\nabla_{\text{U}}^2 \Phi(\mathbf{x}) = a^{-2} \sum_{\mathbf{i}} [\Phi(\mathbf{x} + a\mathbf{i}) - 2\Phi(\mathbf{x}) + \Phi(\mathbf{x} - a\mathbf{i})], \quad (2.2)$$

where the sum is over unit vectors in the three lattice directions: $(1,0,0)$, $(0,1,0)$, and $(0,0,1)$. We use instead a standard improvement, which approaches the continuum Laplacian faster for smooth fields:

$$\nabla_{\text{I}}^2 \Phi(\mathbf{x}) = a^{-2} \sum_{\mathbf{i}} \left[-\frac{1}{12} \Phi(\mathbf{x} + 2a\mathbf{i}) + \frac{4}{3} \Phi(\mathbf{x} + a\mathbf{i}) - \frac{15}{2} \Phi(\mathbf{x}) + \frac{4}{3} \Phi(\mathbf{x} - a\mathbf{i}) - \frac{1}{12} \Phi(\mathbf{x} - 2a\mathbf{i}) \right]. \quad (2.3)$$

The difference can be seen from the Fourier transforms of the operators ∇_{U}^2 and ∇_{I}^2 , which are

$$\tilde{k}_{\text{U}}^2 \equiv a^{-2} \sum_i (2 - 2 \cos(ak_i)), \quad (2.4)$$

$$\tilde{k}_{\text{I}}^2 \equiv a^{-2} \sum_i \left(\frac{5}{2} - \frac{8}{3} \cos(ak_i) + \frac{1}{6} \cos(2ak_i) \right), \quad (2.5)$$

and have small k limits

$$\tilde{k}_{\text{U}}^2 = k^2 + O(a^2 k^4), \quad (2.6)$$

$$\tilde{k}_{\text{I}}^2 = k^2 + O(a^4 k^6). \quad (2.7)$$

The unimproved Laplacian has $O(a^2)$ error while the improved Laplacian has only $O(a^4)$ errors.

A. An unimproved calculation of $\Delta\langle\phi\rangle^2$

One of our tasks is to calculate the continuum ratio $\Delta\langle\phi^2\rangle/u$. In the lattice theory (2.1), the free field ($u_0 = 0$) result for $\langle\Phi^2\rangle$ is

$$\langle\Phi^2\rangle_{u_0=0} = \langle\Phi_1^2 + \Phi_2^2\rangle_{u_0=0} = 2 \int_{\mathbf{k}\in\text{BZ}} \frac{1}{\tilde{k}^2}, \quad (2.8)$$

where the integral is over the Brillouin zone $|k_i| \leq \pi/a$. Scaling out the dependence on a , we define

$$\frac{\Sigma}{4\pi a} \equiv \int_{\mathbf{k}\in\text{BZ}} \frac{1}{\tilde{k}^2}. \quad (2.9)$$

For the improved Laplacian, we obtain the value of the constant Σ by numerical integration:

$$\Sigma \simeq 2.75238391120752. \quad (2.10)$$

On the lattice, the most straightforward implementation of the ratio $\Delta\langle\phi^2\rangle/u$ is then

$$\frac{\Delta_0\langle\Phi^2\rangle}{u_0} \equiv \frac{1}{u_0} \left[\langle\Phi^2\rangle - \frac{2\Sigma}{4\pi a} \right]. \quad (2.11)$$

This will approach the desired continuum value as $ua \rightarrow 0$, but the lattice spacing errors at small ua will be $O(ua)$.

B. Relationship between lattice and continuum fields and parameters

One of our goals will be to reduce finite lattice spacing errors, so that we can obtain better estimates of the continuum limit with a given coarseness of lattice. To eliminate errors at a given order in a , one must not only improve the form of the Laplacian but must also perform an appropriate calculation of the relationship between lattice and continuum parameters. To this end, we will rewrite our bare lattice action in terms of continuum fields ϕ and parameters (r, u) as

$$\mathcal{L} = a^3 \sum_{\mathbf{x}} \left[\frac{Z_\phi}{2} (-\phi_1 \nabla_{\text{lat}}^2 \phi_1 - \phi_2 \nabla_{\text{lat}}^2 \phi_2) + \frac{Z_r(r + \delta r)}{2} (\phi_1^2 + \phi_2^2) + \frac{u + \delta u}{4!} (\phi_1^2 + \phi_2^2)^2 \right], \quad (2.12)$$

where the renormalizations Z_ϕ , Z_r , δr , and δu depend on r and u . We explain their derivation in Appendix B. For continuum r defined by $\overline{\text{MS}}$ renormalization at a scale $\bar{\mu}$, we find

$$Z_\phi = 1 + \frac{2C_2}{9} \frac{(ua)^2}{(4\pi)^2} + O((ua)^3), \quad (2.13a)$$

$$Z_r = 1 + \frac{2\xi}{3} \frac{ua}{(4\pi)} + \left(\frac{4\xi^2}{9} - \frac{2C_1}{3} \right) \frac{(ua)^2}{(4\pi)^2} + O((ua)^3), \quad (2.13b)$$

$$\delta r = a^{-2} \left[-\frac{2\Sigma}{3} \frac{(ua)}{(4\pi)} + \frac{2}{9} \left(\ln \frac{6}{\bar{\mu}a} + C_3 - 3\Sigma\xi \right) \frac{(ua)^2}{(4\pi)^2} + O((ua)^3) \right], \quad (2.13c)$$

$$\delta u = a^{-1} \left[\frac{5\xi}{3} \frac{(ua)^2}{(4\pi)} + \left(-\frac{32C_1}{9} + \xi^2 \right) \frac{(ua)^3}{(4\pi)^2} + O((ua)^4) \right], \quad (2.13d)$$

where we have introduced several new numerical constants, given by various integrals in lattice perturbation theory, whose values (for the action with the improved Laplacian) are approximately

$$\xi \simeq -0.083647053040968, \quad (2.14a)$$

$$C_1 \simeq 0.0550612, \quad (2.14b)$$

$$C_2 \simeq 0.033416, \quad (2.14c)$$

$$C_3 \simeq -0.86147916. \quad (2.14d)$$

One needs to similarly match the operator ϕ^2 whose expectation is taken in determining $\Delta\langle\phi^2\rangle$. In Appendix B, we discuss the relationship between the continuum and lattice operators and show that the continuum result for $\Delta\langle\phi^2\rangle$ is

$$\Delta\langle\phi^2\rangle = Z_r\langle\phi^2\rangle_{\text{lat}} - \delta\phi^2 + O(a^2), \quad (2.15)$$

where the constant $\delta\phi^2$ is

$$\delta\phi^2 = a^{-1} \left\{ \frac{2\Sigma}{4\pi} + \frac{4\xi\Sigma}{3} \frac{ua}{(4\pi)^2} + \frac{4}{9} [C_4 - 3\Sigma C_1 - \Sigma C_2 + 2\xi^2\Sigma + \xi \ln(\bar{\mu}a)] \frac{(ua)^2}{(4\pi)^3} - \xi \frac{ra^2}{4\pi} \right\}. \quad (2.16)$$

The new numerical constant is

$$C_4 \simeq 0.282. \quad (2.17)$$

In this paper, whenever we quote simulation results for a given value of ua and ra^2 , we are referring to simulations of the action (2.12) with parameters given by (2.13) and (2.15) with $O(\dots)$ set to zero. When we quote values of $\Delta\langle\phi^2\rangle_c$, we will be quoting continuum values, as given by (2.15). This will be adequate to reduce the lattice spacing error to $O(a^2)$ on individual measurements of $\Delta\langle\phi^2\rangle_c/u$ and to $O(a)$ on individual measurements r_c . In fact, as discussed in Appendix B, the order of our expansions (2.13) for Z_ϕ , Z_r , and δu are formally overkill for this purpose, but we've used the full expansion anyway for reasons having to do with other applications.

The precise definition of continuum r , and its relationship to bare lattice r_0 , are in principle unnecessary if one's interest is only to determine $\Delta\langle\phi^2\rangle_c$ — one could simply find the critical value of r_0 at any given lattice spacing and not worry about its relation to continuum definitions. However, as a practical matter, knowing the relationship facilitates using results at one lattice spacing to make a good initial guess of the critical value of r_0 at a new lattice spacing. And, as discussed earlier, the continuum critical value of r is of interest in its own right.

Throughout this paper, continuum r should be understood as defined by $\overline{\text{MS}}$ renormalization at a renormalization scale $\bar{\mu}$. That is, the continuum Lagrangian is the $\epsilon \rightarrow 0$ limit of the $(3-\epsilon)$ -dimensional action

$$S = \int d^{3-\epsilon}x \left[Z_\phi(\nabla\phi)^* \cdot (\nabla\phi) + r_{\text{bare}}\phi^*\phi + \mu^\epsilon \frac{u_{\text{eff}}}{6} (\phi^*\phi)^2 \right], \quad (2.18)$$



FIG. 1. The two fundamental UV-divergent graphs of continuum ϕ^4 theory.

with the bare continuum parameter r_{bare} related to the renormalized $r = r_{\overline{\text{MS}}}(\bar{\mu})$ by

$$r_{\text{bare}} = r + \frac{1}{(4\pi)^2 \epsilon} \left(\frac{u}{3}\right)^2, \quad (2.19)$$

and with

$$\mu \equiv \frac{e^{\gamma_E/2}}{\sqrt{4\pi}} \bar{\mu}. \quad (2.20)$$

[The factor of $e^{\gamma_E/2}/\sqrt{4\pi}$ in (2.20) is what distinguishes modified minimal subtraction ($\overline{\text{MS}}$) from unmodified minimal subtraction (MS); the difference between the two schemes amounts to nothing more than a multiplicative redefinition of the renormalization scale. The constant $\gamma_E = 0.5772 \dots$ is Euler's constant.] Three-dimensional ϕ^4 theory is super-renormalizable and the only fundamental UV divergences of the continuum theory are those corresponding to the two diagrams of fig. 1. The first has a linear divergence, which is ignored by dimensional regularization. The second has a logarithmic divergence, which is the origin of the u^2/ϵ counter-term present in (2.19).

C. Algorithm

We evolve configurations in Monte Carlo time using a combination of site by site heatbath and multi-grid [7] over-relaxation updates.

In section III, we discuss how we define a nominal value of the location r_c of the transition in finite volume. In order to scan for the transition, we need to be able to smoothly vary r . We use the standard technique of canonical reweighting. Having made a simulation at one value r_0 of r , and accumulated a Monte Carlo time series of values of

$$\overline{\phi^2} \equiv \frac{1}{V} \int d^3x \phi^2(\mathbf{x}), \quad (2.21)$$

expectations at nearby values $r = r_0 + \delta r$ can be calculated as

$$\langle \mathcal{O} \rangle_r = \frac{\langle \exp\left(-\frac{1}{2}V \delta r \overline{\phi^2}\right) \mathcal{O} \rangle_{r_0}}{\langle \exp\left(-\frac{1}{2}V \delta r \overline{\phi^2}\right) \rangle_{r_0}}. \quad (2.22)$$

We estimate our statistical errors for the estimates of r_c and $\Delta\langle\phi^2\rangle_c$ in a given simulation run using the jackknife method. That is, we divide the time series into N_{bin} consecutive bins, and perform N_{bin} fits to the data, each with one bin of data missing. The error in a quantity

is estimated as $\sqrt{\sigma^2(N_{\text{bin}} - 1)}$, where σ^2 is the variance of those N_{bin} different measurements of that quantity. The size of each bin must be large compared to the decorrelation time. In practice, we chose $N_{\text{bin}} = 20$ and checked that our estimates are not very sensitive to doubling N_{bin} .

III. FINDING THE CRITICAL POINT

Systems only have sharply defined phase transitions in infinite volume, but we use the method of Binder cumulants [8] to obtain a good estimate, in finite volume simulations, of the critical value r_c of r . Specifically, we measure the cumulant

$$C = \frac{\langle \bar{\phi}^4 \rangle}{\langle \bar{\phi}^2 \rangle^2} \quad (3.1)$$

as a function of r , where the 2-component vector $\bar{\phi}$ is the volume average of ϕ :

$$\bar{\phi} \equiv \frac{1}{V} \int d^3x \phi(\mathbf{x}). \quad (3.2)$$

In infinite volume, the cumulant C is 1 in the ordered phase and 2 in the disordered phase. In large volume, there is a smooth transition between these two values, and the width of the transition region shrinks as the volume is increased. Specifically, for an $L \times L \times L$ volume, the width in r of the transition region scales as L^{-y_t} in the $L \rightarrow \infty$ limit, where $y_t = 1/\nu$ and ν is the correlation-length critical exponent. The value of the exponent is

$$y_t \equiv 1/\nu \approx 1.49 \quad (3.3)$$

for the universality class of the O(2) model.¹

One method of estimating the location of the transition in finite volume is to simply choose a fixed value C_* of C between 1 and 2 and then define the nominal r_c in finite volume as the r for which $C(r) = C_*$. This leads to errors in r_c (contributing to errors in other quantities measured at the transition) that would scale away as L^{-y_t} in the large L limit. This L^{-y_t} scaling of finite-size errors is typical of many prescriptions for defining r_c in finite volume.

The method of Binder cumulants improves the scaling of the finite-size error in r_c from L^{-y_t} to $L^{-y_t - \omega}$, where ω is the critical exponent associated with corrections to scaling, and

$$\omega \simeq 0.79 \quad (3.4)$$

¹ The value of roughly 1.5 comes from the scaling relationship $\nu = (2 - \alpha)/d$ and the fact that the specific heat critical exponent α is very small in this universality class. The best value of α is -0.01285(38) and comes from experiments in Earth orbit on superfluid He⁴ [13]. For comparison, theoretical values (making use of $\alpha = 2 - d\nu$ as necessary) are $\alpha = -0.011(4)$, $-0.004(11)$, and $-0.0169(9)(24)$ from 3D series techniques [14], the ϵ expansion [14], and Monte Carlo [9].

for the universality class of the $O(2)$ model.² One version of the method is to measure the curves $C(r)$ for two different large system sizes L_1 and L_2 , and then estimate r_c as the point r_\times where the curves intersect. Specifically, Binder [8] showed that, in the $L_1, L_2 \rightarrow \infty$ limit, the error scales as

$$r_\times(L_1, L_2) - r_c \sim \frac{L_2^{-\omega} - L_1^{-\omega}}{L_1^{y_t} - L_2^{y_t}} = \frac{b^{-\omega} - 1}{1 - b^{y_t}} L_1^{-y_t - \omega}, \quad (3.5)$$

where $b \equiv L_2/L_1$. Moreover, the value of the cumulant C_\times at the intersection approaches a *universal* value C_c in this limit, with corrections scaling as

$$C_\times(L_1, L_2) - C_c \sim \frac{L_1^{y_t} L_2^{-\omega} - L_2^{y_t} L_1^{-\omega}}{L_1^{y_t} - L_2^{y_t}} = \frac{b^{-\omega} - b^{y_t}}{1 - b^{y_t}} L_1^{-\omega} \quad (3.6)$$

for $L_1, L_2 \rightarrow \infty$. This last result is a simple consequence of Binder's analysis [8], but, for the sake of completeness, we briefly outline the argument in Appendix D.

If one knew C_c in advance, then, for data in a given finite volume, a nice method for determining a nominal point of transition is to choose the r such that $C(r) = C_c$. The finite size error in r_c caused by this procedure also scales as $L^{-y_t - \omega}$. This method is simpler and statistically a little cleaner than trying to find the intersection of two $C(r)$ curves for two different values of L . This is the method we shall use, but first we need a value of C_c .

We would like to choose L as large as possible, in order to make the scaling law (3.6) as accurate as possible, so that we can use it to extrapolate a good value of C_c . Our ultimate interest in this paper is to study continuum $O(2)$ theory, which requires $ua \ll 1$ and for which the scaling limit is $L/a \gg 1/ua$. But $L/a \gg 1/ua$ implies that small ua simulations are an inefficient choice for getting as far as possible into the scaling limit. Because C_c is universal, we can extract it from large ua simulations rather than small ua simulations. [In fact we could use any model in the same universality class.] In actuality, our simulation code is optimized to perform best if ua is not extremely large, and so we have chosen to extract C_c from data taken with $u_0a = 60$, which we shall see later is a moderate large value of ua . Because $u_0a = 60$ is not a small value of ua , the $O(a)$ improvements to the action are pointless; unlike other simulations reported in this paper, we quote quantities in terms of the bare lattice parameters.

Fig. 2 shows the intersecting $C(r)$ curves for $u_0a = 60$ simulations for a variety of system sizes. A variety of intersection values $C_\times(L_1, L_2)$ are plotted in Fig. 3 against $(L_1^{y_t} L_2^{-\omega} - L_2^{y_t} L_1^{-\omega}) / (L_1^{y_t} - L_2^{y_t})$ which, by (3.6), should lead to a linear relationship at large L_1, L_2 . The errors on points sharing an L value are correlated, and we compute and use the full correlation matrix for making fits. For the sake of simplicity, however, we have only fit the subset of data with $L_1 = 2L_2$, with results for C_c and the associated confidence levels given in Table I. We take as our final result

$$C_c = 1.234 \pm 0.002. \quad (3.7)$$

² Values are $\omega = 0.789(11)$, $0.802(18)$, and $0.79(2)$ from 3D series techniques [14], the ϵ expansion [14], and Monte Carlo [9].

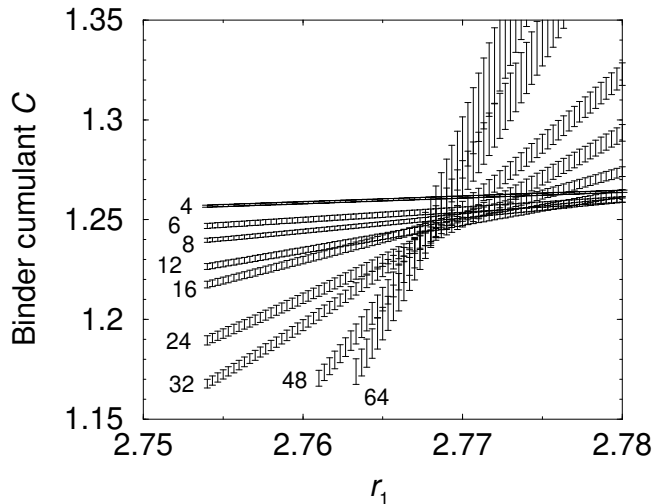


FIG. 2. Intersections of cumulant curves $C(r)$ for various system sizes L at $u_0a = 60$ (unimproved). Each curve is labelled by L/a . The horizontal axis shows $r_1 \equiv r_0 - \Sigma u/6\pi a$, which is the bare lattice parameter r_0 shifted by the tadpole correction. Within each volume, the statistical errors shown are very highly correlated.

fit	C_c	C.L.
$L_2/a \geq 24$	1.241(56)	NA
$L_2/a \geq 16$	1.220(20)	70%
$L_2/a \geq 12$	1.235(11)	64%
$L_2/a \geq 8$	1.236(4)	82%
$L_2/a \geq 6$	1.235(4)	92%
$L_2/a \geq 4$	1.2352(26)	96.5%
$L_2/a \geq 3$	1.2341(17)	97.3%

TABLE I. Results of linear fits to the subset of data of fig. 3 with $L_1 = 2L_2$, and the corresponding confidence levels (“NA” means not applicable). The first row corresponds to a fit to two points, the second to three points, etc. We believe that the somewhat high confidence levels in the last lines are coincidental.

This result is close to a rough³ estimate of $C_c \simeq 1.243$ provided by the simulation results of Ref. [9].

In the rest of this paper, when quoting results for the transition in a given finite volume, we will mean the point where

³ We call this estimate rough because computing C_c was not a goal of Ref. [9], and they did not provide an analysis of systematic errors. Specifically, they quote a fairly accurate result for the $L \rightarrow \infty$ value of the C at which $\xi_{2nd}/L = 0.5927$, where ξ_{2nd} is a length defined in terms of the ratio of the correlator at momenta 0 and $2\pi/L$. However, the number 0.5927 is quoted as coming from preliminary studies, and they make no firm statement about how accurately 0.5927 corresponds to the “critical” value of this parameter (defined by the $L \rightarrow \infty$ limit of its value at precisely r_c), nor how any inaccuracy would translate into uncertainty in C_c . For their purpose, which was to calculate the scaling exponent ω from simulations, a precise correspondence is inessential.

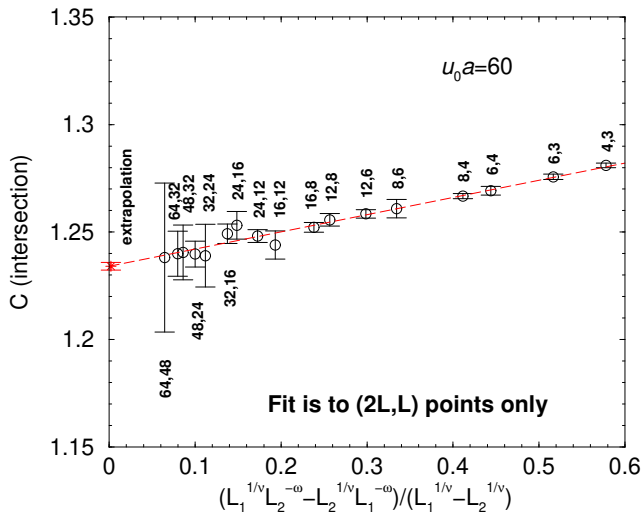


FIG. 3. The values $C_{\times}(L_1, L_2)$ corresponding to the intersection points of pairs of the curves shown in Fig. 2. The horizontal axis has been chosen so that this relationship should be linear as $L_1, L_2 \rightarrow \infty$ (which corresponds to approaching zero on the horizontal axis). Each point is labeled by L_1/a and L_2/a . The linear fit shown is only to that subset of points with $L_1 = 2L_2$.

$$C(r) = 1.234 \quad (3.8)$$

for that volume, and we will ignore the error in our determination of C_c . We have checked that this error contributes a negligible error to our final results (1.4) and (1.5). Specifically, changing C_c by the error we quote in (3.7) and repeating the analysis of this paper changes our final results by roughly one tenth of their quoted error.

IV. VOLUME DEPENDENCE OF $\Delta\langle\phi^2\rangle_c$

As discussed in the introduction, the only parameter of the continuum problem at the critical point is u . So the only length scale of the problem is $1/u$. The relevant measure of the size L of a finite-volume lattice relative to this scale is therefore Lu (and similarly the relevant measure of lattice spacing is ua). Fig. 4 shows a plot of our results for $\Delta\langle\phi^2\rangle_c$ on $L \times L \times L$ lattices vs. Lu for $ua = 6$. As can be seen, our largest Lu values are clearly large: the data clearly shows nice convergence towards an infinite volume limit. To understand the size of the remaining finite-volume error, we will want to fit the volume dependence at large Lu to an appropriate scaling law.

A. Large volume scaling of $\Delta\langle\phi^2\rangle_c$

The scaling of large L corrections depends on universal critical exponents of the $O(2)$ model, which is in the same universality class as the classical $N = 2$ Heisenberg ferromagnet. The language of critical exponents in the $O(2)$ model is borrowed from correspondence with the Heisenberg magnet, and $t \equiv r - r_c$ is referred to as the reduced “temperature” in this context, $C \propto d^2(\ln Z)/dt^2$ as the “specific heat,” and so forth. It is important to emphasize

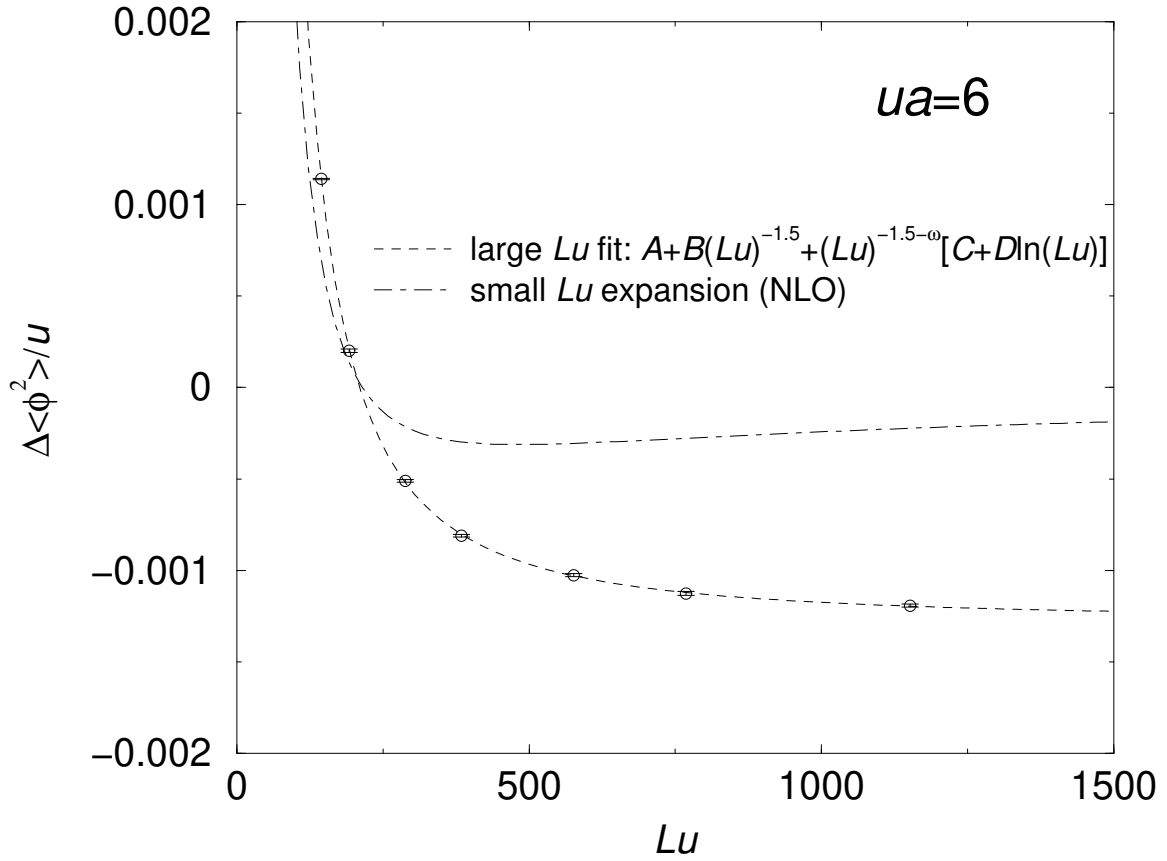


FIG. 4. Simulation results for $\Delta\langle\phi^2\rangle_c/u$ vs. lattice size in physical units (Lu) for $ua = 6$. The large Lu curve shown is a fit to all but the leftmost data point, with confidence level 33%.

that this language holds the potential for confusion because, in many applications (such as Bose-Einstein condensation at fixed density), $t \equiv r - r_c$ is not, in fact, linearly related to the actual temperature of the system near the critical point, and $d^2(\ln Z)/dt^2$ is not directly the physical specific heat.⁴ In any case, the analog of the “energy density” E/V under this correspondence is

$$\frac{E}{V} \propto \frac{d(\ln Z)}{V dt} = \frac{1}{V} \frac{d}{dr} \ln \int [\mathcal{D}\phi] e^{-S[\phi]} \propto \langle \phi^2 \rangle, \quad (4.1)$$

where $V = L^d$ is the system volume and $d = 3$ is the dimension. The problem of understanding how the finite volume corrections to $\langle \phi^2 \rangle$ scale with L can therefore be stated in this language as the problem of how corrections to the “energy density” scale with L for anything in this universality class.

The standard finite-size scaling ansatz provided by renormalization group methods is that the free energy density $f = -V^{-1} \ln Z$ scales as⁵

$$f(t, \{u_j\}, L^{-1}) = f_{\text{reg}}(t, \{u_j\}) + b^{-d} f_{\text{sing}}(b^{y_t} t, \{u_j b^{y_j}\}, b/L) \quad (4.2)$$

for periodic boundary conditions, where f_{reg} and f_{sing} generate the so-called regular and singular parts of the free energy in the infinite volume limit. (See Refs. [11,12] and references therein.) The length b is an arbitrary renormalization scale (block size), and $\{u_j\}$ denotes the set of infrared-irrelevant operators (with corresponding $y_j < 0$). Standard notation for critical exponents is $\nu = 1/y_t$, and we will denote the smallest $|y_j|$ associated with the irrelevant operators $\{u_j\}$ as ω .

Choosing $b = L$,

$$f(t, u_j, L^{-1}) = f_{\text{reg}}(t, u_j) + L^{-d} f_{\text{sing}}(L^{y_t} t, u_j L^{y_j}, 1). \quad (4.3)$$

The usual infinite-volume scaling form is obtained by taking $L \rightarrow \infty$ with t fixed, which, for the limit to exist, requires

$$f_{\text{sing}}(\tau, 0, 1) \sim \tau^{-d/y_t} \quad \text{as} \quad \tau \rightarrow \infty. \quad (4.4)$$

In contrast, for fixed L , the free energy will be analytic in t , since there are no phase transitions in finite volume. We can make a Taylor expansion of the finite-volume free energy (4.3) in t (as well as $\{u_j L^{y_j}\}$), which should be a useful expansion when the arguments of the scaling piece f_{sing} are small. That is, for situations where $L^{y_t} t \rightarrow 0$ as we take $L \rightarrow \infty$, we can Taylor expand (4.3) as

⁴ A uniform, non-relativistic Bose gas is a constrained system: the particle density n is fixed. This constraint causes a different relationship of model parameters and the physical temperature than for unconstrained systems [10]. For example, the critical exponents $\tilde{x} = (\tilde{\alpha}, \tilde{\beta}, \tilde{\gamma}, \tilde{\nu})$ of the actual system are related to the standard exponents $x = (\alpha, \beta, \gamma, \nu)$ of the field theory by (i) $\tilde{\alpha} = -\alpha/(1 - \alpha)$, and $\tilde{x} = x/(1 - \alpha)$ for the others, if $\alpha > 0$, or (ii) $\tilde{x} = x$ if $\alpha < 0$. This relation explains the difference between mean-field theory exponents for the O(2) model (e.g. $\alpha = 1/2$) and the exponents of a non-interacting Bose gas (e.g. $\tilde{\alpha} = -1$).

⁵ We have not included a “magnetic field” h coupling to ϕ , with a corresponding argument $b^{y_h} h$ in f_{sing} , because we will only be interested in the case $h = 0$ and are not interested in correlations of ϕ (as opposed to ϕ^2), which could be generated by derivatives with respect to h .

$$\begin{aligned}
f &= (A_0 + B_0 L^{-d} + C_0 L^{-d-\omega}) + \dots \\
&+ t(A_1 + B_1 L^{-d+y_t} + C_1 L^{-d+y_t-\omega} + \dots) \\
&+ t^2(A_2 + B_{20} L^{-d+2y_t} + \dots) \\
&+ \dots,
\end{aligned} \tag{4.5}$$

where we have only displayed the leading corrections due to irrelevant operators. Differentiating with respect to t to get the energy density, we find that $\langle \phi^2 \rangle$ scales in large volume as

$$\begin{aligned}
\langle \phi^2 \rangle &= (A_1 + B_1 L^{-d+y_t} + C_1 L^{-d+y_t-\omega} + \dots) \\
&+ 2t(A_2 + B_{20} L^{-d+2y_t} + \dots) + \dots.
\end{aligned} \tag{4.6}$$

As mentioned earlier, use of the method of Binder cumulants to determine r_c means that, in our application,

$$t \sim L^{-y_t-\omega}. \tag{4.7}$$

This indeed satisfies the condition $L^{y_t} t \rightarrow 0$ as $L \rightarrow 0$, and so the expansion (4.6) is appropriate. For our application, we then have

$$\langle \phi^2 \rangle = A_1 + B_1 L^{-d+y_t} + A'_2 L^{-y_t-\omega} + C'_1 L^{-d+y_t-\omega} + \dots. \tag{4.8}$$

Using the standard scaling relation $\alpha = 2 - \nu d$ for the specific heat scaling exponent α , this can be rewritten in the form

$$\langle \phi^2 \rangle = A_1 + B_1 L^{-(1-\alpha)y_t} + A'_2 L^{-y_t-\omega} + C'_1 L^{-(1-\alpha)y_t-\omega} + \dots. \tag{4.9}$$

The value of α in the three-dimensional O(2) model is very small: $\alpha \simeq -0.013$, corresponding to the value $y_t \simeq 1.49$ quoted earlier.⁶

The renormalizations Z_r and $\delta\phi^2$ that convert $\langle \phi^2 \rangle_{\text{lat}}$ into $\Delta\langle \phi^2 \rangle$ in (2.15) do not introduce any new powers of L , and so the form of the large- L expansion of $\Delta\langle \phi^2 \rangle$ is the same as that for $\langle \phi^2 \rangle$ in (4.9) above, though the coefficients are different.

B. Large volume scaling for $\alpha = 0$

Because we do not have large volume data spanning many decades in L , α is zero for all practical purposes. And so one might as well use the $\alpha = 0$ limit of the large-volume scaling (4.9), which corresponds to $y_t = d/2$. Typically, $\alpha = 0$ generates logarithms in an RG analysis, which can appear as a superposition

$$\lim_{\alpha \rightarrow 0} \frac{s^{z+q\alpha} - s^z}{\alpha} = qs^z \ln s \tag{4.10}$$

⁶ See footnote 1 for references.

of power laws $s^{z+q\alpha}$ and s^z for some variable of interest s . One might therefore expect that the $\alpha \rightarrow 0$ limit of the large-volume scaling (4.9) is

$$\langle \phi^2 \rangle = A_1 + B_1 L^{-d/2} + L^{-d/2-\omega} (C \ln L + D) + \dots \quad (4.11)$$

It's useful to verify the presence of a logarithm. If it weren't there, we could include the first corrections to scaling in large L fits of our data using a 3-parameter fit $[A_1, A_2, D]$ rather than a 4-parameter fit $[A_1, B_1, C, D]$; or equivalently A_1, B_1, A'_2, C'_1 in (4.9).

The existence of the logarithm can be directly related to the well known logarithmic divergence of specific heat with t when $\alpha = 0$. We give a renormalization group analysis in Appendix C that makes this explicit. Here, let us just note that the logarithm follows from an old proposal by Privman and Rudnick [15]. Ignore corrections to scaling for the moment, and suppose that at $\alpha = 0$ the free energy had the general form (4.3) discussed earlier:

$$f(t, L^{-1}) \sim f_{\text{reg}}(t) + L^{-d} f_{\text{sing}}(tL^{d/2}). \quad (4.12)$$

In order to get a logarithmic divergence $\ln(t^{-1})$ of the specific heat in the infinite volume limit, we need a term $t^2 \ln(t^{-1})$ in the free energy in that limit. So we must have

$$f_{\text{sing}}(\tau) \sim A\tau^2 \ln(\tau^{-1}) \quad \text{as} \quad \tau \rightarrow \infty. \quad (4.13)$$

But this would give $f \sim f_{\text{reg}}(t) + At^2 \ln(t^{-1}L^{-d/2})$, which doesn't have a good $L \rightarrow \infty$ limit. The solution is to suppose that the $\alpha = 0$ version of the free energy is instead

$$f(t, L^{-1}) \sim f_{\text{reg}}(t) + At^2 \ln(L^{d/2}) + L^{-d} f_{\text{sing}}(tL^{d/2}), \quad (4.14)$$

which is what Privman and Rudman proposed. Note that the new term is analytic as $t \rightarrow 0$ for L fixed, as it must be. The new term gives a $t \ln L$ contribution to the energy density E/V , which, for the $t \sim L^{-y_t-\omega}$ of interest to us, gives rise to the logarithm term in (4.11).

C. How large is large volume?

Before proceeding to numerical fits of the large volume dependence, it is useful to first have an idea of how large L should be before one might reasonably hope for large volume scaling to hold. From Fig. 4, we see that the finite volume corrections to the continuum value of $\Delta\langle\phi^2\rangle_c$ become 100% where the data crosses zero, at roughly $Lu \sim 200$. So one might guess that this is very roughly the scale where scaling starts to set in—the scale that separates short-distance perturbative physics from long-distance critical-scaling physics. We can check this rough assessment from the other side. In the limit of small Lu , the physics of fluctuations is perturbative, and one can analytically compute the expected value of $\Delta\langle\phi^2\rangle_c$ order by order in powers of Lu . We perform this computation in Appendix E in the continuum ($ua = 0$) to next-to-leading order (NLO) in Lu , with the result that

$$\frac{\Delta\langle\phi^2\rangle_c}{u} = \frac{6.61341}{(Lu)^{3/2}} - \frac{0.451570}{Lu} + O((Lu)^{-1/2}) \quad (4.15)$$

for our critical value (3.8) of the Binder cumulant. The resulting curve is shown in both figs. 4 and 5 (as well as the leading-order small Lu result in fig. 5). One can see that the

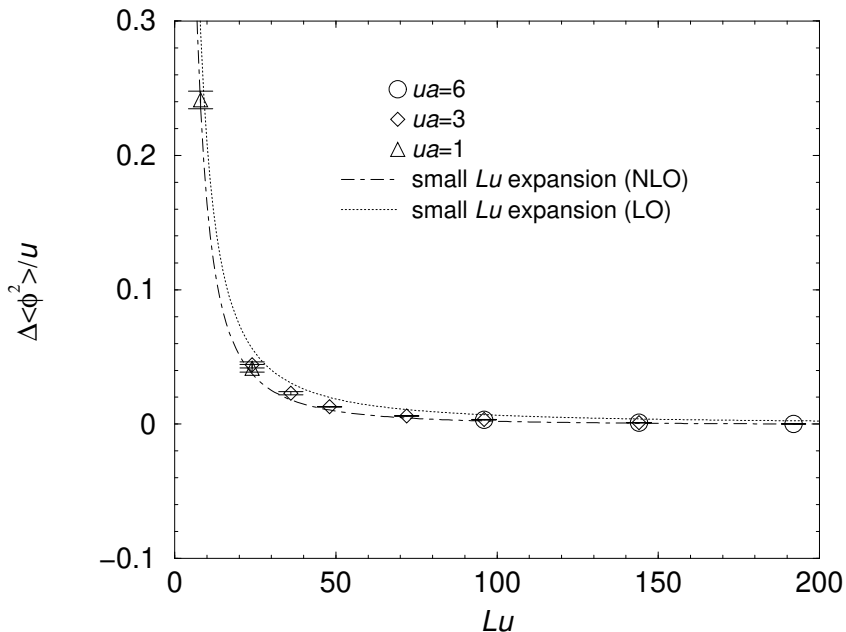


FIG. 5. Simulation results for $\Delta\langle\phi^2\rangle_c/u$ vs. lattice size, showing more small volume data than Fig. 4. The dot-dash curve shows the next-to-leading order small Lu expansion of (4.15). The dotted curve shows just the leading-order term of that expansion.

small Lu expansion becomes unreliable past $Lu \sim 200$, which is the same as the previous scale estimate.

Interestingly, the scale $Lu \sim 200$ is close to what one might estimate on the back of an envelope from a large- N approximation to the theory. In large N , one replaces the $O(2)$ theory studied here by an $O(N)$ theory of N scalar fields and solves the theory in the approximation that N is large—a program pursued for the problem of Bose-Einstein condensation of a non-relativistic gas in Refs. [16,17]. In the $N \rightarrow \infty$ limit, one introduces an auxiliary field σ whose propagator represents a geometric sum of bubble diagrams, such as shown in fig. 6. The corresponding resummed propagator is proportional to

$$\frac{1}{\frac{3}{Nu} + \tilde{\Sigma}_0(p)}, \quad (4.16)$$

where $\tilde{\Sigma}_0(p)$ represents the basic massless bubble integral

$$\tilde{\Sigma}_0(p) \equiv \frac{1}{2} \int_l \frac{1}{l^2 |l + \mathbf{p}|^2} = \frac{1}{16p}. \quad (4.17)$$

The propagator (4.16) changes from its large momentum behavior (\rightarrow constant) to its small momentum behavior ($\propto p$) at a scale given by $3/Nu \sim \Sigma_0(p)$. This corresponds to $p \sim Nu/48$ and so distance scales of order $L \sim 2\pi/p \sim 96\pi/Nu$. Setting $N = 2$, we find $Lu \sim 48\pi \sim 150$. Of course, one would never hope an estimation this crude to be useful beyond, at best, the factor of 2 level.

Our discussion of system size has implications for the validity of an early numerical study of the critical temperature for Bose-Einstein condensation for non-relativistic gases [18]. We discuss this in Appendix F.

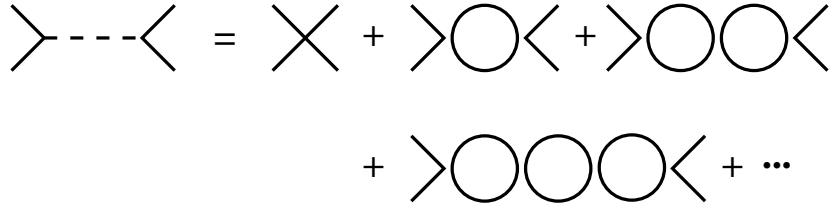


FIG. 6. Bubble chains, which are the source of scale dependence in large N calculations of $\Delta\langle\phi^2\rangle_c$ in $O(N)$ theory [16,17].

V. NUMERICAL EXTRAPOLATION OF $Lu \rightarrow \infty$

A. Extrapolating $\Delta\langle\phi^2\rangle_c$ to $Lu \rightarrow \infty$

We now examine fits of the $ua=6$ data of Fig. 4 to the large L scaling form of (4.11). Figs. 7 and 8 show the results of extrapolating to $L \rightarrow \infty$ under various assumptions, using various subsets of the data. The squares refer to fits to (4.11), which includes corrections to scaling. The circles correspond to fitting only the leading-order scaling corrections (that is, ignoring the sub-leading terms, which involve the exponent ω). For comparison, the diamonds show what happens if we ignore finite-size effects altogether, and the corresponding confidence levels are terrible. Also for comparison, the triangles show what happens if we ignore the logarithmic dependence in the corrections to scaling. For the fits with reasonable confidence levels, these points are not too different from the full form given by the squares. The vertical dashed line in Fig. 4 marks the moderate system size $L = 150$ (discussed in the previous section), below which you should become suspicious of any attempt to fit the data to a large-volume scaling form.

A simple method for assigning a final result for the extrapolation is to take our best fit with a correct scaling form. As seen in Fig. 7, the leading-order scaling form $A + BL^{-d/2}$ is perfectly adequate for fitting our large Lu data. We take as our estimate the 75% confidence level fit to $Lu \geq 384$, which gives

$$\left[\frac{\Delta\langle\phi^2\rangle_c}{u} \right]_{ua=6} = -0.001287(9), \quad (5.1)$$

which is depicted by the shaded region of Figs. 7 and 8.

As described in Ref. [1], we will actually use $Lu = 576$ as a reference point from which to derive finite volume and finite lattice spacing corrections. Figs. 9 and 10 are similar to figs. 7 and 8 but shows the size of the finite-size correction at $Lu = 576$, as determined by the fit. The best fit (the 75% confidence level one) gives

$$\left[\frac{\Delta\langle\phi^2\rangle_c}{u} \right]_{Lu=576} - \left[\frac{\Delta\langle\phi^2\rangle_c}{u} \right]_{Lu \rightarrow \infty} = 0.000258(7). \quad (5.2)$$

As we shall see, $ua = 6$ is a reasonably small value of ua , and we expect this to be a good estimate to the finite volume corrections in the continuum ($ua \rightarrow 0$) limit.

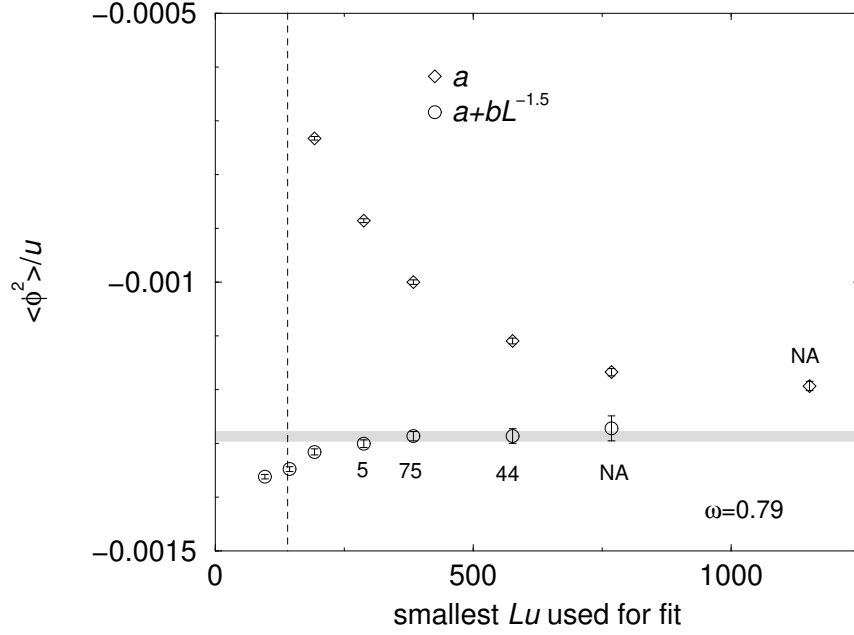


FIG. 7. Extrapolations of the $ua=6$ data of Fig. 4 to $L \rightarrow \infty$ under various assumptions of the functional form. The horizontal axis shows the smallest value of Lu of the data used for the fit. Percentage confidence levels are written next to each extrapolation whenever non-negligible ($\geq 1\%$), and “NA” (not applicable) refers to those cases where the number of data points used for the fit equals the number of parameters.

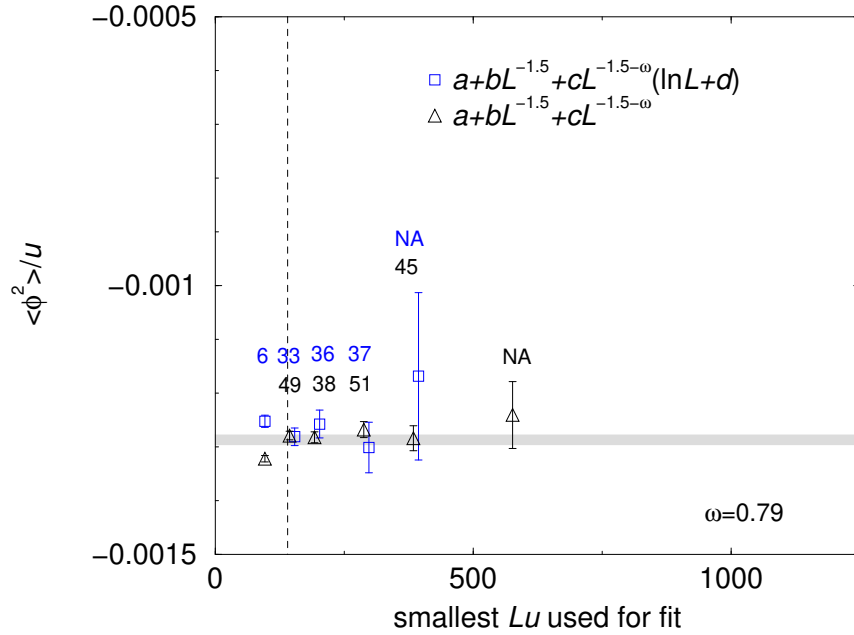


FIG. 8. As Fig. 8 but showing extrapolations that include corrections to scaling. Where two confidence levels are listed on top of each other, the upper one is for the square data point and the lower for the triangular data point.

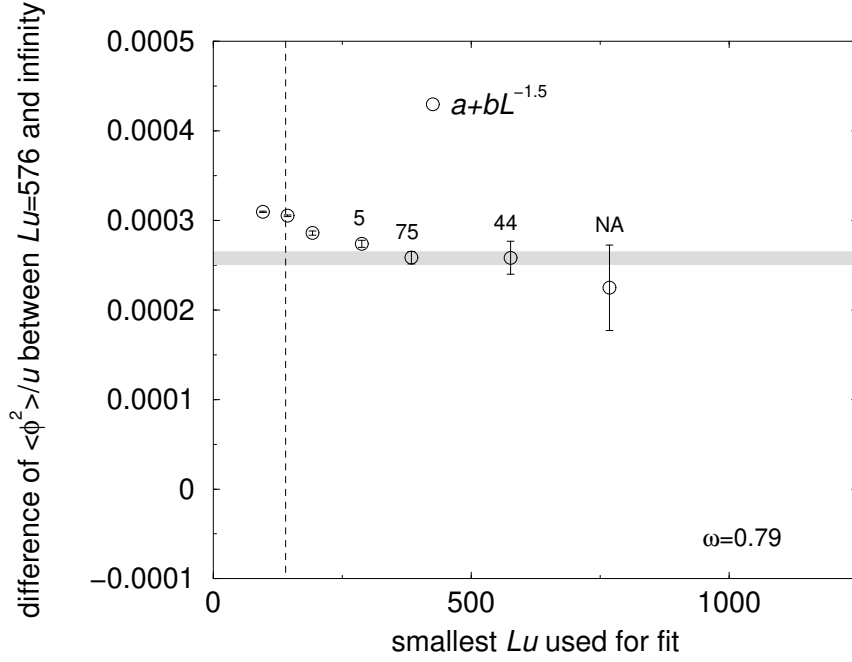


FIG. 9. As Fig. 7 but shows the magnitude of the finite-size correction to $\Delta\langle\phi^2\rangle_c/u$ at $Lu = 576$, as determined by the fit.

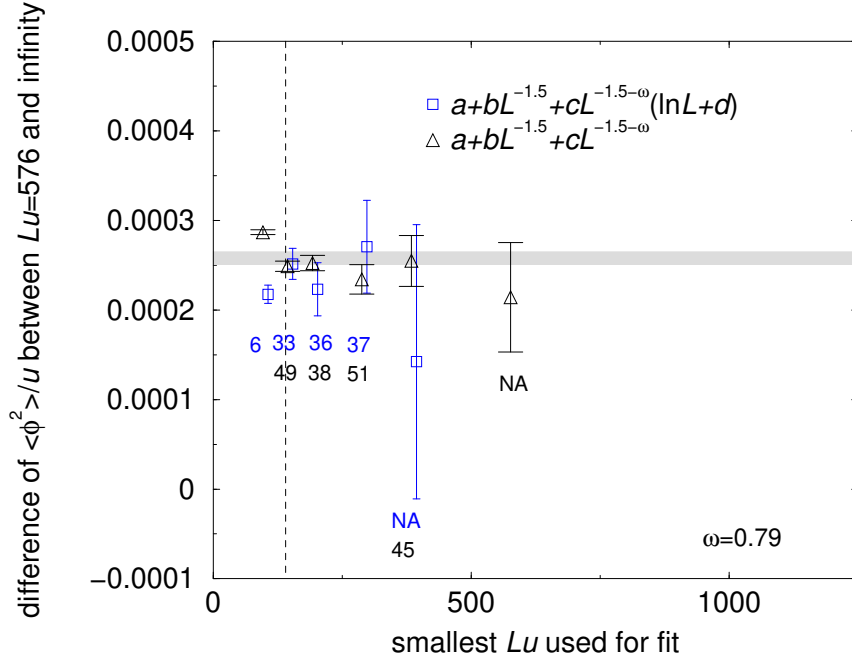


FIG. 10. As Fig. 8 but shows the magnitude of the finite-size correction to $\Delta\langle\phi^2\rangle_c/u$ at $Lu = 576$, as determined by the fit.

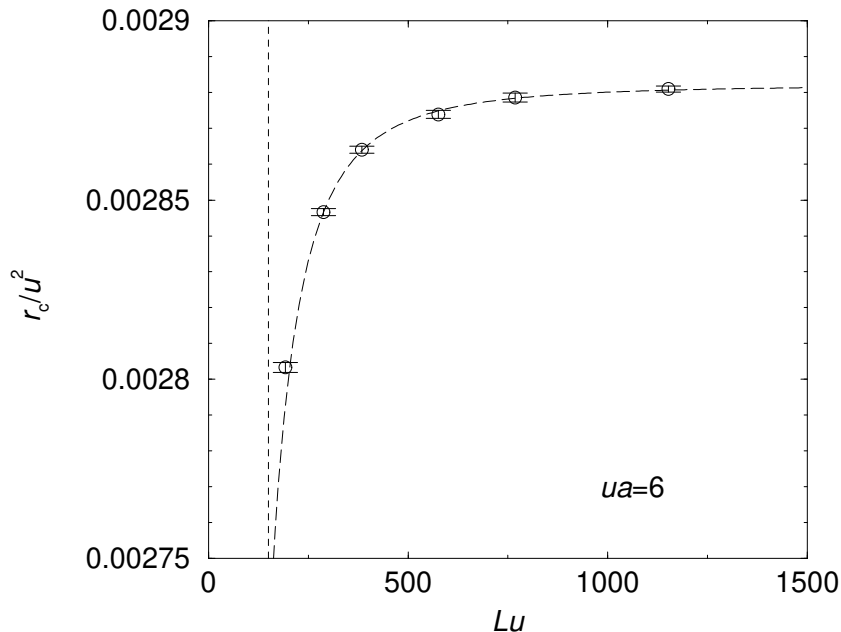


FIG. 11. $ua = 6$ data for the nominal value of r_c/u^2 (defined in $\overline{\text{MS}}$ renormalization at renormalization scale $\bar{\mu} = u/3$) as a function of system size. The fit shown by the dashed line is the large-volume fit to all but the leftmost data point.

B. Extrapolating r_c to $Lu \rightarrow \infty$

We will now make a similar analysis of finite-size effects for the critical value r_c of r . The continuum value of r is convention dependent—it depends on one’s choice of renormalization scheme and renormalization scale. As discussed earlier, our convention will be to define r with $\overline{\text{MS}}$ regularization at the renormalization scale $\bar{\mu} = u/3$. The conversion formula (1.6) to other choices of $\bar{\mu}$ can be extracted from (2.13c) and the fact that the theory is super-renormalizable.

Fig. 11 shows, for $ua = 6$, the dependence on system size of our finite-volume determinations of $r_c(u/3)/u^2$. As discussed in section III, the finite-size corrections are expected to scale as $L^{-\omega}$ as $L \rightarrow \infty$. Fig. 12 shows the result of extrapolating an infinite-volume result by fitting various subsets of the data to $A + BL^{-\omega}$. There are two results with roughly 80% confidence level, and we take the one fitting the most data points:

$$\left[\frac{r_c(u/3)}{u^2} \right]_{ua=6} = 0.0028822(7). \quad (5.3)$$

Fig. 13 shows the size of the finite volume error at our canonical $Lu = 576$, as determined by the fits,

$$\left[\frac{r_c(u/3)}{u^2} \right]_{Lu=576} - \left[\frac{r_c(u/3)}{u^2} \right]_{Lu=\infty} = -0.00000726(26). \quad (5.4)$$

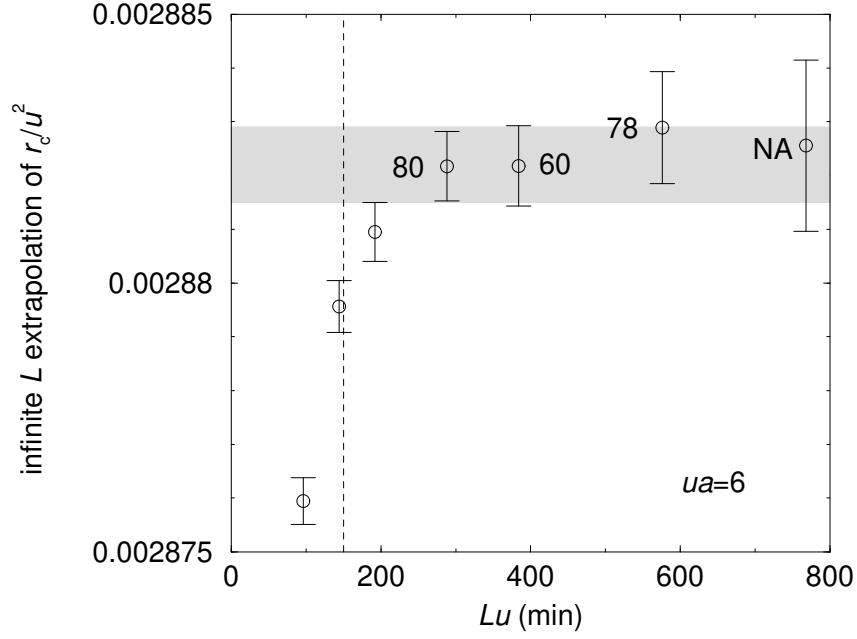


FIG. 12. Extrapolations of the $ua=6$ data of Fig. 11 to $L \rightarrow \infty$ using the functional form $A + BL^{-y_t - \omega}$. The horizontal axis shows the smallest value of Lu of the data used for the fit. Confidence levels are written as described for Fig. 7.

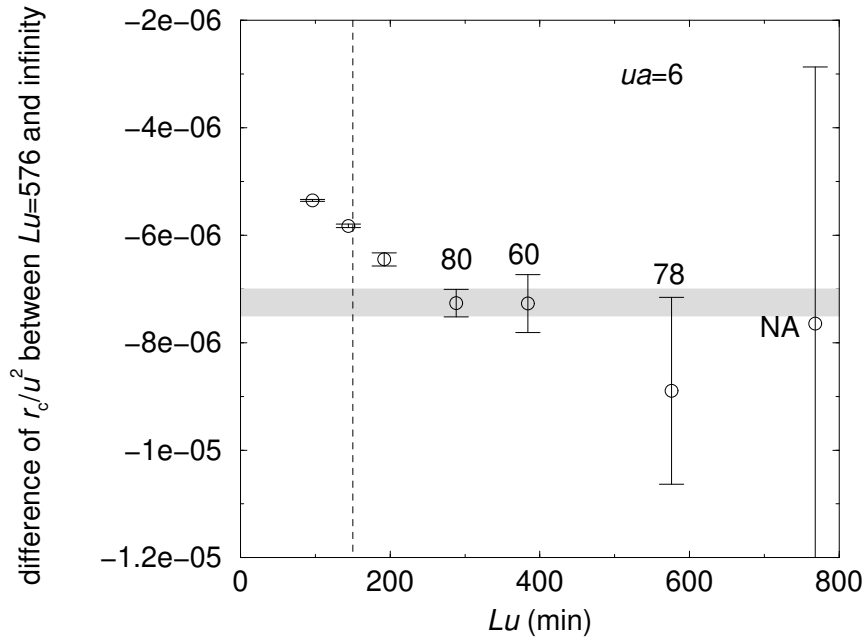


FIG. 13. As fig. 12 but showing the magnitude of the finite-size correction to r_c/u^2 at $Lu = 576$.

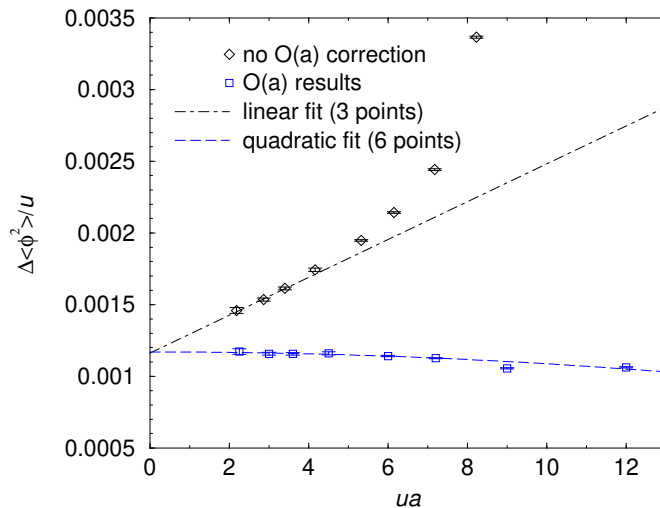


FIG. 14. The squares show results for $\Delta\langle\phi^2\rangle_c/u$ vs. ua at $Lu = 144$. The line through them is a fit of the first 6 points to $A + B(ua)^2$. The diamonds represent the corresponding uncorrected data, as described in the text, and a straight line has been fit through the first three points.

VI. NUMERICAL EXTRAPOLATION OF $ua \rightarrow 0$

A. Extrapolating $\Delta\langle\phi^2\rangle_c$ to $ua \rightarrow 0$

We will now discuss numerical results for the continuum limit $a \rightarrow 0$ while holding the physical volume of the lattice fixed. This can be expressed as $ua \rightarrow 0$ holding Lu fixed. Since the number $(L/a)^3$ of lattice sites we can practically include in a simulation is limited, we can obviously explore smaller values of ua when we fix smaller values of Lu . As a test that we understand our lattice spacing errors, we have therefore made several simulations at the rather moderate system size of $Lu = 144$ (see the discussion of sec. IV C). The results for the dependence of $\Delta\langle\phi^2\rangle_c/u$ on ua are shown by the squares in Fig. 14. If our corrections for $O(a)$ errors have been calculated correctly, the remaining error should be $O(a^2)$. Indeed, all but the largest ua data point in Fig. 14 fit very well the functional form $A + B(ua)^2$, with confidence level 92%.

It's interesting to compare to what would have been obtained if we had used the same data but instead plotted the uncorrected

$$\frac{\Delta\langle\Phi^2\rangle_c}{u_0} = \frac{1}{u_0} \left[\langle\Phi^2\rangle - \frac{\Sigma}{2\pi a} \right] \quad (6.1)$$

vs. u_0a , where Φ and u_0 are the bare lattice fields and coupling of (2.1). This uncorrected data is represented by the diamonds in Fig. 14. One clearly sees the $O(a)$ corrections. We should make clear that this is still $Lu = 144$ data and is not $Lu_0 = 144$ data, which would have required additional simulations.

Fig. 15 shows the ua dependence at a reasonably large physical system size of $Lu = 576$. We show extrapolations of the $ua \rightarrow 0$ limit in fig. 16. Here, the 10% confidence levels of fits to $A + B(ua)^2$ are less spectacular than the $Lu = 144$ data, though not unreasonable.

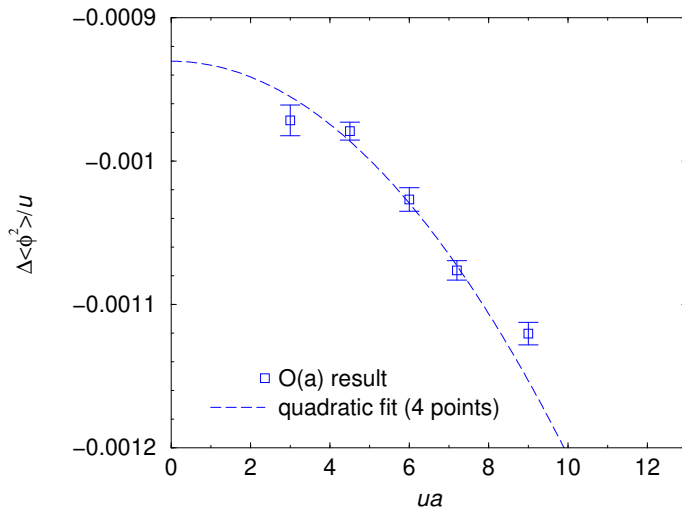


FIG. 15. Results for $\Delta\langle\phi^2\rangle_c/u$ vs. ua at $Lu = 576$. The line is a fit of $A + B(ua)^2$ to all but the rightmost data point.

Because of the lower confidence levels, we have been a little more conservative in our error estimate. We take as our result for the $ua \rightarrow 0$ limit the shaded region of fig. 16, which has been chosen to cover both the 10–15% confidence level fits:

$$\left[\frac{\Delta\langle\phi^2\rangle_c}{u^2} \right]_{Lu=576} = -0.000937(15). \quad (6.2)$$

Combining this with the finite volume correction (5.2), and adding errors in quadrature, we arrive at our final value (1.4) for the infinite-volume continuum limit. Note that the dominant error in this estimate comes from the $ua \rightarrow 0$ extrapolation.

B. Extrapolating r_c to $ua \rightarrow 0$

Fig. 17 shows the dependence of r_c on ua at the medium system size of $Lu = 144$, where we can simulate down to relatively small values of ua . The data fits well to a linear dependence on ua , with the fit shown to the first six points in the figure having a 43% confidence level. A similar plot for the reasonably large system size of $Lu = 576$ is shown in Fig. 18. The corresponding extrapolations to $ua = 0$ based on linear fits are shown in fig. 19. We take the $ua = 0$ extrapolation to be

$$\left[\frac{r_c(u/3)}{u^2} \right]_{Lu=576} = 0.0019119(20), \quad (6.3)$$

as shown by the shaded region of the figure. Combining with our estimate (5.4) of the finite size error at $Lu = 576$ gives our final result (1.5) for the infinite-volume continuum limit. Again, the dominant error comes from the $ua \rightarrow 0$ extrapolation.

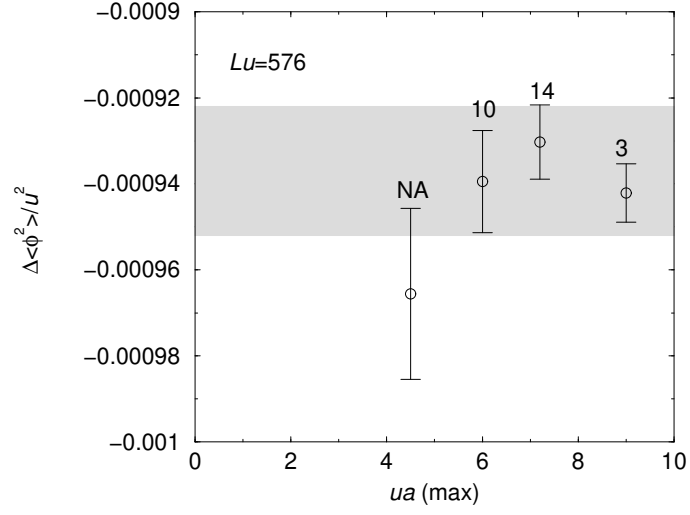


FIG. 16. Extrapolations of the data of Fig. 15 to $ua = 0$ fitting to the form $A + B(ua)^2$. The horizontal axis shows the maximum value of ua used for each fit. Confidence levels are written as described for Fig. 7.

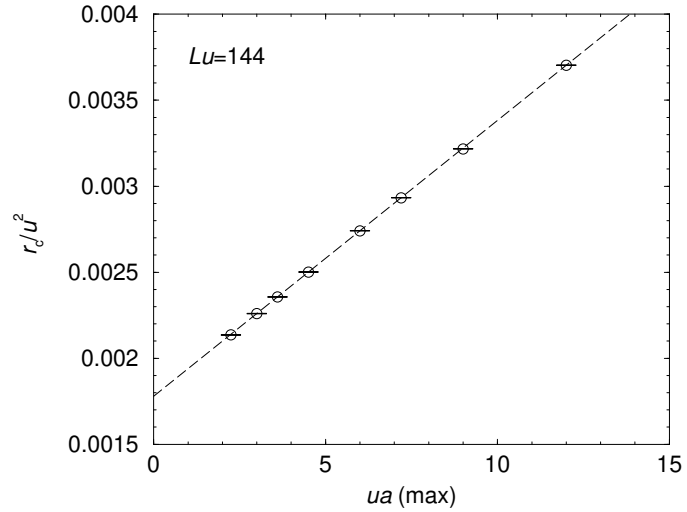


FIG. 17. Results for r_c/u^2 vs. ua at $Lu = 144$ (defined in $\overline{\text{MS}}$ renormalization at renormalization scale $\bar{\mu} = u/3$). The line is a linear fit.

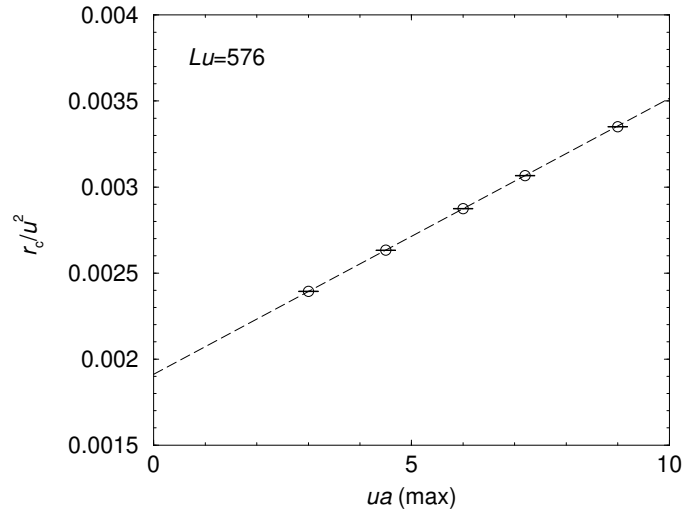


FIG. 18. Results for r_c/u^2 vs. ua at $Lu = 576$ (defined in $\overline{\text{MS}}$ renormalization at renormalization scale $\bar{\mu} = u/3$). The line is a linear fit.

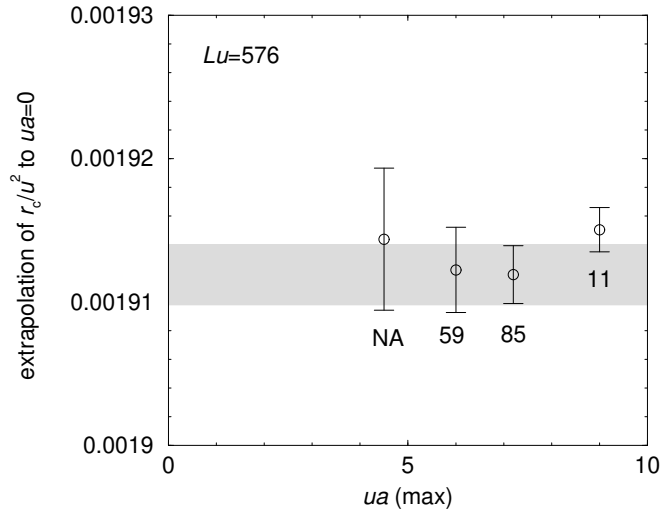


FIG. 19. Linear extrapolations of the data of Fig. 18 to $ua = 0$. The horizontal axis shows the maximum value of ua used for each fit. Confidence levels are written as described for Fig. 7.

ACKNOWLEDGMENTS

We are indebted to John Cardy for outlining to us the argument of appendix C. This work was supported by the U.S. Department of Energy under Grant Nos. DE-FG03-96ER40956 and DE-FG02-97ER41027.

APPENDIX A: TABULATED DATA

Lu	ua	L/a	$\Delta\langle\phi^2\rangle_c/u$	r_c/u^2
8	1	8	0.2412(66)	-0.0316(11)
24	1	24	0.0416(29)	-0.00233(37)
24	3	8	0.0441(23)	-0.00283(27)
36	3	12	0.0229(11)	0.00007(14)
48	3	16	0.01291(10)	0.001136(12)
72	3	24	0.00607(16)	0.001856(25)
96	3	32	0.003456(69)	0.0020683(78)
96	6	16	0.0033126(92)	0.0025643(12)
144	2.25	64	0.001172(19)	0.0021356(25)
144	3	48	0.001157(10)	0.0022599(16)
144	3.6	40	0.0011566(85)	0.00235635(96)
144	4.5	32	0.001160(10)	0.0025015(14)
144	6	24	0.0011406(46)	0.00274092(61)
144	7.2	20	0.0011262(41)	0.00293273(70)
144	9	16	0.0010551(46)	0.00321670(59)
144	12	12	0.0010621(46)	0.00370381(51)
192	6	32	0.0002011(91)	0.0028033(14)
288	6	48	-0.0005105(76)	0.0028467(10)
384	3	128	-0.0007130(56)	0.00237986(91)
384	4	96	-0.000764(11)	0.0025456(15)
384	4.8	80	-0.0007699(81)	0.0026718(14)
384	6	64	-0.0008103(70)	0.00286403(99)
384	8	48	-0.0008782(81)	0.0031835(12)
384	12	32	-0.01174(18)	0.0038320(18)
576	3	192	-0.000972(11)	0.0023935(16)
576	4.5	128	-0.0009790(63)	0.00263301(78)
576	6	96	-0.0010267(82)	0.0028739(11)
576	7.2	80	-0.0010761(68)	0.00306619(94)
576	9	64	-0.0011202(78)	0.0033505(11)
768	6	128	-0.001127(11)	0.0028786(12)
1152	6	192	-0.0011982(95)	0.00288184(96)
1152	6	192	-0.001168(23)	0.0028785(16)

APPENDIX B: MATCHING CONTINUUM AND LATTICE THEORIES

1. General discussion

In this appendix we discuss the $O(a)$ and $O(a^2)$ improvement of three-dimensional scalar field theory on the lattice. For the sake of generality, and because it is not any harder, we will discuss $O(N)$ scalar field theory of N real fields $\phi = (\phi_1, \phi_2, \dots, \phi_N)$. The case of interest to the present work is $N = 2$. As in (2.12), the lattice Lagrangian is defined to be

$$\mathcal{L} = a^3 \sum_{\mathbf{x}} \left[\frac{Z_\phi}{2} \sum_{i=1}^N (-\phi_i \nabla_{\text{lat}}^2 \phi_i) + \frac{Z_r(r + \delta r)}{2} \phi^2 + \frac{u + \delta u}{4!} (\phi^2)^2 \right], \quad (\text{B1})$$

where

$$\phi^2 \equiv \sum_{i=1}^N \phi_i^2, \quad (\text{B2})$$

and ϕ , r , and u are just the (UV renormalized) continuum fields and parameters in lattice units. So $\phi_{\text{lat}} = a^{1/2} \phi_{\text{cont}}$, $u_{\text{lat}} = au_{\text{cont}}$, and $r_{\text{lat}} = a^2 r_{\text{cont}}$. Of these, r_{cont} is the only continuum parameter that requires UV renormalization and should be understood as renormalized with dimensional regularization and the $\overline{\text{MS}}$ scheme. In this appendix, we will calculate, to a given order in lattice spacing, the necessary counter-terms Z_ϕ , Z_r , δr , and δu required to implement this correspondence between continuum and lattice variables. To match the lattice and continuum theories to high orders in a , we would need to include other operators in our lattice theory, such as ϕ^6 , $\phi^2 |\nabla \phi|^2$, and so forth. However, these will turn out to be unnecessary at the order to which we will work.

A given local lattice action will never perfectly reproduce the continuum action. For small ua , the error in how a given lattice action treats physics at the distance scale a can be computed and compensated for by perturbative calculations. The discrepancy in how a given lattice action, with given parameters, treats the non-perturbative physics at the distance scale $1/u$ cannot. It is therefore important that the lattice action be close enough to the continuum action that errors at the scale $1/u$ are higher order in a than whatever is desired. In order to improve our simulations and measurement of $\Delta \langle \phi^2 \rangle_c$ to $O(a)$ accuracy, it is necessary to (a) match the lattice action and parameters so that, at the scale $1/u$, it reproduces the physics of the continuum action up to and including $O(a)$; and (b) match the lattice and continuum definitions of operator ϕ^2 to the same order, so that the measurements of $\Delta \langle \phi^2 \rangle_c$ will match up. Actually, the first requirement is slightly overstated. To measure $\Delta \langle \phi^2 \rangle_c$ to $O(a)$, it is not necessary to match the lattice and continuum parameters r to that order. That's because, in the simulations, we will simply vary the coefficient of ϕ^2 in the action until we find the transition – we don't need to know its relation to r_{cont} to do this.

In this appendix, we will match r_{cont} to the lattice just to $O(a^0)$. This will make possible a determination of the continuum value of the critical value r_c , but $O(a)$ errors will remain and must be removed by extrapolation to the continuum limit. We will match the continuum and lattice definitions of the operator ϕ^2 through $O(a)$, so that we can make an $O(a)$ improved calculation of $\langle \phi^2 \rangle_c$. For the sake of other applications, we will match the lattice action through $O(a^2)$ [except for the matching of r just discussed], even though a matching to $O(a)$ would be adequate for our purposes here.

At tree level, the infrared behavior of the lattice and continuum theories are the same up to corrections suppressed by at least a^2 ; the power of a can be higher if we choose the lattice ∇^2 appropriately. However there are “radiative” corrections induced in the IR physics by the nonlinearity of the theory, together with the UV difference between the lattice and continuum theories. The diagrams of Fig. 20, for instance, differ on the lattice from their continuum values because the dispersion relations of the scalar fields differ in the UV, and the loop momentum integration integrates over this region. These effects are suppressed by powers of the couplings; the radiative correction to the scalar 4 point function, for instance,

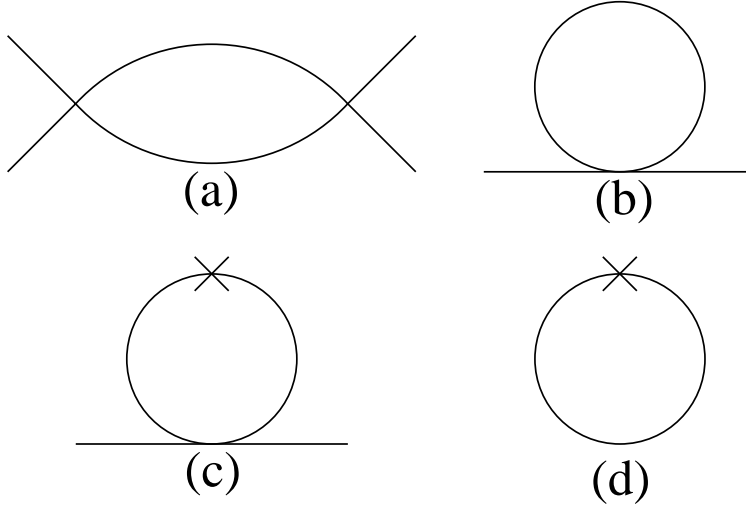


FIG. 20. The one loop graphs needed for the renormalization. A cross represents a ϕ^2 insertion, which in turn could represent either (i) a perturbative insertion of the $r\phi^2$ term of the action or (ii) the ϕ^2 operator associated with calculating the expectation $\langle\phi^2\rangle$.

clearly depends on u^2 . On dimensional grounds, the difference between lattice and continuum values of this diagram must go as u^2a , so these diagrams lead to $O(a)$ differences between the lattice and continuum theories. The difference between lattice and continuum values of these diagrams can be removed by a renormalization of the parameters of the lattice theory.

As discussed in the main text, we will be interested not only in how to renormalize the parameters of the action but also in how to translate expectation values of the operator ϕ^2 between the lattice and continuum. It will be convenient to talk directly about the operator ϕ^2 , which is associated with UV divergences in the continuum, rather than $\Delta\langle\phi^2\rangle$, which is not. We will define ϕ^2 in the continuum also using $\overline{\text{MS}}$ renormalization. In general, operators with the same symmetry can mix under renormalization, and the lattice operator ϕ^2 will correspond to some superposition of the unit continuum operator, the renormalized ϕ^2 continuum operator, and higher-dimensional renormalized continuum operators such as ϕ^4 :

$$a^{-1}(\phi^2)_{\text{lat}} = c_0 + c_2(\phi^2)_{\text{cont}} + c_4(\phi^4)_{\text{cont}} + \dots \quad (\text{B3})$$

However, our particular interest is in expectation values at the transition. For this application, the effects of higher-and-higher dimensional operators on the right-hand side of (B3) become suppressed by more and more powers of ua . For example, c_2 is $O(1)$, and the expectation value of the renormalized continuum operator ϕ^2 is, by dimensional analysis, $O(u)$ at the transition. So the $c_2(\phi^2)_{\text{cont}}$ term contributes $O(u)$ to the expectation. In contrast, the lowest-order diagram that contributes to mixing between ϕ^2 and ϕ^4 is shown in Fig. 21 and gives $c_4 = O(u^2a^3)$ above, where the u^2 counts the two vertices in Fig. 21 and the a^3 then follows by dimensional analysis. But, also by dimensional analysis, the renormalized continuum expectation $\langle\phi^4\rangle$ is $O(u^2)$. So the $c_4(\phi^4)_{\text{cont}}$ term contributes $O(u^4a^3)$ to the expectation, down by three powers of ua from $c_2(\phi^2)_{\text{cont}}$. Our goal will be to compute the $O(a)$ corrections to $\Delta\langle\phi^2\rangle_c$, for which it is therefore adequate to compute just c_0 and c_2 above.

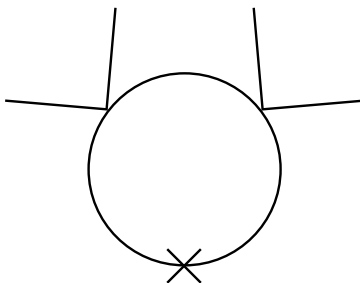


FIG. 21. A diagram contributing to the mixing of the ϕ^2 and ϕ^4 operators.

The diagrams which contribute to c_2 are the same as those which contribute to the multiplicative renormalization of the coefficient r of ϕ^2 in the action, and $1/c_2$ is the same as the Z_r introduced previously. Rearranging the terms in (B3), we will write

$$a(\phi^2)_{\text{cont}} = Z_r(\phi^2)_{\text{lat}} - \delta\phi^2 + O((ua)^4), \quad (\text{B4})$$

where $\delta\phi^2$ represents a c -number (ac_0/c_2) parameterizing mixing with the unit operator, which we shall calculate.

We will see later that, for the purpose of calculating the $O(a)$ corrections to $\Delta\langle\phi^2\rangle_c$, all that is strictly required is one-loop results for Z_ϕ , Z_r , δu , and δr , and three-loop results for $\delta\phi^2$. To determine r_c [just at $O(a^0)$] requires tree results for Z_ϕ , δu , and Z_r , and two-loop results for δr . However, for the sake of other applications, we will include here two-loop determinations of Z_ϕ , δu , and Z_r and have incorporated them into our action, as described in the main text. If one made a three-loop computation of δr (which we have not), one could obtain the $O(a)$ corrections for r_c as well.

Now we turn to the calculations. For the remainder of this appendix, we will work exclusively in lattice units ($a = 1$).

2. One-loop results

A one loop renormalization calculation will determine the $O(a)$ contributions to the quantities Z_ϕ , δu , and Z_r , and will find the $O(1/a)$ contributions to δm^2 and $\delta\langle\phi^2\rangle$. The details of the power counting used here can be found in [19]. In the small lattice spacing limit, the momentum scale $r^{1/2}$ associated with the parameter r is small compared to the scale $1/a$ where the lattice and continuum theories differ. So, for the specific purpose of a calculation to match the lattice and continuum theories, the $r\phi^2$ term in the action (as well as the $u\phi^4$ term) may be treated perturbatively.

The required graphs are shown in Figure 20. Evaluating the graphs requires choosing a lattice Laplacian, and for completeness we will consider both the unimproved (2.2) and improved (2.3) choices described in the main text. The evaluation of the one loop graphs requires two integrals:

$$\frac{\Sigma}{4\pi} \equiv \int_{\text{BZ}} \frac{d^3k}{(2\pi)^3} \frac{1}{\bar{k}^2}, \quad (\text{B5})$$

$$\frac{\xi}{4\pi} \equiv \int_{\text{BZ}} \frac{d^3k}{(2\pi)^3} \frac{1}{(\tilde{k}^2)^2} - \int_{\mathbb{R}^3} \frac{d^3k}{(2\pi)^3} \frac{1}{k^4}. \quad (\text{B6})$$

Here we use the shorthand BZ to mean k lies within the Brillouin zone, meaning each $k_i \in [-\pi, \pi]$. The notation \tilde{k}^2 is introduced in Eq. (2.4). The integrals which determine ξ are each IR singular and some regulation is implied, for instance adding m^2 to both k^2 and \tilde{k}^2 and taking the limit as $m^2 \rightarrow 0$. The numerical values of the integrals, accurate to ± 1 in the last digit, are ⁷

$$\begin{aligned} \Sigma_{\text{U}} &= 3.17591153562522, & \Sigma_{\text{I}} &= 2.75238391130752, \\ \xi_{\text{U}} &= 0.152859324966101, & \xi_{\text{I}} &= -0.083647053040968. \end{aligned} \quad (\text{B7})$$

Note that the sign of ξ depends on whether we use an improved lattice Laplacian. This is possible because ξ represents the difference of a graph between lattice and continuum theories. The lattice contribution is larger inside the Brillouin zone, but the continuum integral receives contributions from outside the zone as well; the sign depends on which effect is larger.

At one loop the renormalizations are (in lattice units)

$$\delta u_{1l} = \frac{(N+8)}{6} \frac{\xi}{4\pi} u^2, \quad (\text{B8})$$

$$Z_{\phi,1l} - 1 = 0, \quad (\text{B9})$$

$$Z_{r,1l} - 1 = \frac{(N+2)}{6} \frac{\xi}{4\pi} u, \quad (\text{B10})$$

$$\delta r_{1l} = -\frac{(N+2)}{6} \frac{\Sigma}{4\pi}, \quad (\text{B11})$$

$$\delta \phi_{1l}^2 = N \frac{\Sigma}{4\pi}. \quad (\text{B12})$$

3. Two-loop results

For the renormalizations Z_{ϕ} and Z_r , it makes no sense to carry the renormalization to two loops unless we use the improved lattice Laplacian, because already at tree level the unimproved Laplacian gives $O(a^2)$ level errors in the propagator. The two loop results require several more graphs as well as the inclusion in one-loop graphs of one-loop mass and coupling counterterms. (See Figure 22.) Four more integrals are needed, which we will evaluate in a moment. The complete 2-loop result for general N is

$$\delta u_{2l} - \delta u_{1l} = \left[\frac{(N^2 + 6N + 20)}{36} \left(\frac{\xi}{4\pi} \right)^2 - \frac{(5N + 22)}{9} \frac{C_1}{(4\pi)^2} \right] u^3, \quad (\text{B13})$$

⁷ An analytic result [6] for Σ_{U} is $\frac{8}{\pi}(18 + 12\sqrt{2} - 10\sqrt{3} - 7\sqrt{6})[\mathbf{K}((2 - \sqrt{3})^2(\sqrt{3} - \sqrt{2})^2)]^2$, where \mathbf{K} is the complete elliptic integral of the first kind.

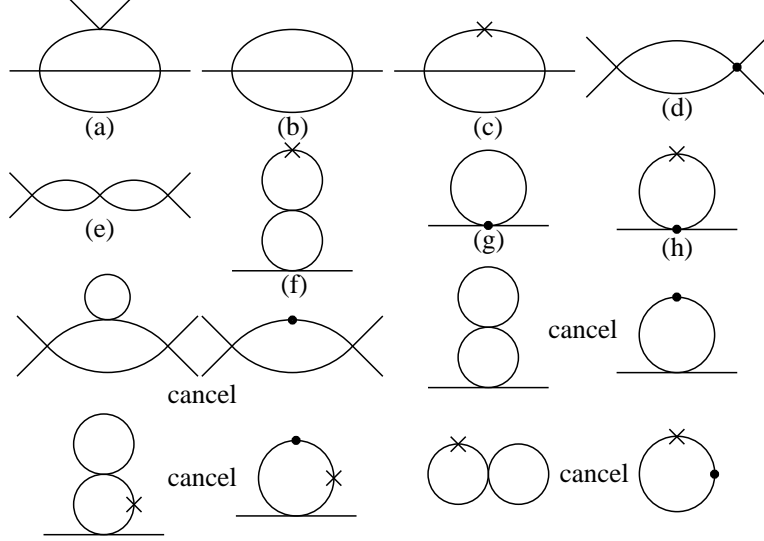


FIG. 22. All required two loop graphs and one loop graphs with one loop counterterm insertions, shown as heavy dots on lines (mass counterterms) or at vertices (coupling counterterms). The last eight graphs cancel in pairs. Diagrams (a), (d), and (e) are not separately IR convergent; diagram (d) must be distributed between the other two to produce IR convergent integrals.

$$Z_{\phi,2l} - 1 = \frac{(N+2)}{18} \frac{C_2}{(4\pi)^2} u^2, \quad (\text{B14})$$

$$Z_{r,2l} - Z_{r,1l} = \left[\left(\frac{N+2}{6} \right)^2 \left(\frac{\xi}{4\pi} \right)^2 - \frac{(N+2)}{6} \frac{C_1}{(4\pi)^2} \right] u^2, \quad (\text{B15})$$

$$\delta r_{2l} - \delta r_{1l} = \frac{(N+2)}{18(4\pi)^2} \left[C_3 + \ln \left(\frac{6}{\bar{\mu}} \right) - 3\Sigma\xi \right] u^2, \quad (\text{B16})$$

$$\delta\phi_{2l}^2 - \delta\phi_{1l}^2 = \frac{N(N+2)}{6} \frac{\Sigma\xi}{(4\pi)^2} u. \quad (\text{B17})$$

The three numerical constants C_1 , C_2 , and C_3 are given for the improved Laplacian in (2.14). Only C_3 can be usefully defined for the unimproved case,⁸ where it is $C_{3,U} = .08848010$.

Now we detail the calculation of the constants C_1 through C_3 . We will use the following shorthands: $\int_{k,\text{BZ}}$ means $\int d^3k/(2\pi)^3$, with range the Brillouin zone $[-\pi, \pi]^3$; whereas \int_{k,\mathbb{R}^3} is the same but integrated over all 3-space. Further, we define the following integrals, which will come up repeatedly:

$$I_L(p) = \int_{q,\text{BZ}} \frac{1}{\tilde{q}^2(p+q)^2}, \quad (\text{B18})$$

$$I_C(p) = \int_{q,\mathbb{R}^3} \frac{1}{q^2(p+q)^2} = \frac{1}{8|p|}. \quad (\text{B19})$$

We begin with the two-loop vertex correction, graph (a) of Figure 22. The required integral, including the appropriate amount of the one loop counterterm graph (d), is

⁸ In ref. [20], this constant is called ζ .

$$\frac{C_1}{(4\pi)^2} = \int_{k,\text{BZ}} \frac{1}{(\tilde{k}^2)^2} \left\{ I_L(k) - \frac{\xi}{4\pi} \right\} - \int_{k,\mathfrak{R}^3} \frac{1}{k^4} I_C(k). \quad (\text{B20})$$

We re-arrange the original integral into three parts,

$$\int_{k,\text{BZ}} \frac{1}{(\tilde{k}^2)^2} \left\{ I_L(k) - \frac{1}{8k} - \frac{\xi}{4\pi} \right\} + \int_{k,\text{BZ}} \frac{1}{8k} \left(\frac{1}{(\tilde{k}^2)^2} - \frac{1}{k^4} \right) - \int_{k,\mathfrak{R}^3 - \text{BZ}} \frac{1}{8k^5}. \quad (\text{B21})$$

All three of the above integrals are convergent, provided we use the improved Laplacian. The first integral is IR well behaved because the two counterterms cancel $I_L(k)$ up to a k^2 correction, which in the small k limit is $I_L(k) - (1/8k) - (\xi/4\pi) \rightarrow .0125438 k^2/4\pi$.

To get accurate numerical answers, we perform all 3-D integrals by quadratures. Dealing with the double poles which appear in I_L is touchy, and requires adaptive mesh refinement techniques. We improve the precision of each final result by repeating the full integration at several spacings and extrapolating (Richardson extrapolation). The first integral in (B21) gives $.0360003/16\pi^2$, and the second gives $.054568958/16\pi^2$. The last integral, over $\mathfrak{R}^3 - \text{BZ}$, can be re-arranged into

$$- \frac{3}{16\pi^5} \int_0^1 dx \int_0^1 dy \frac{1}{(1+x^2+y^2)^{5/2}}, \quad (\text{B22})$$

which can be performed very accurately and gives $-.035507296027\dots/16\pi^2$. These sum to give $C_1 = .0550612$.

Besides this graph, there is graph (e), which gives

$$\left(\int_{k,\text{BZ}} \frac{1}{(\tilde{k}^2)^2} \right)^2 - \left(\int_{k,\mathfrak{R}^3} \frac{1}{k^4} \right)^2, \quad (\text{B23})$$

which is *not* IR convergent. However, including -2 times the counterterm diagram (d),

$$-2 \left(\int_{k,\text{BZ}} \frac{1}{(\tilde{k}^2)^2} \right) \left(\int_{k,\text{BZ}} \frac{1}{(\tilde{k}^2)^2} - \int_{k,\mathfrak{R}^3} \frac{1}{k^4} \right), \quad (\text{B24})$$

gives $-(\xi/4\pi)^2$. No new integrals are required. It is a nontrivial check on the calculation that the sum of the coefficients arising from diagrams (a) and (e) precisely absorb diagram (d).

The next integral is the $O(p^2)$ contribution from the setting sun diagram (b),

$$\frac{C_2}{(4\pi)^2} = \lim_{p \rightarrow 0} \frac{1}{p^2} \left\{ \int_{k,\text{BZ}} \left(\frac{1}{(\widetilde{k+p})^2} - \frac{1}{\tilde{k}^2} \right) I_L(k) - \int_{k,\mathfrak{R}^3} \left(\frac{1}{(k+p)^2} - \frac{1}{k^2} \right) I_C(k) \right\}. \quad (\text{B25})$$

The first trick is to note that

$$\int_{k,\text{BZ}} \left(\frac{1}{(\widetilde{k+p})^2} - \frac{1}{\tilde{k}^2} \right) = 0 \quad (\text{B26})$$

just by shifting the integration variable for the first term. So we may add an arbitrary constant to $I_L(k)$ in (B25), and we choose the constant $-\xi/4\pi$. This will prevent IR divergences

in what follows. We are now free to expand $1/(\widetilde{k+p})^2$ to second order in p . After averaging over directions for p , we find

$$\frac{1}{(\widetilde{k+p})^2} - \frac{1}{\widetilde{k}^2} \rightarrow p^2 \left[\frac{\frac{1}{3} \sum_i \left(\frac{8 \sin k_i - \sin 2k_i}{3} \right)^2}{(\widetilde{k}^2)^3} - \frac{\frac{1}{3} \sum_i \left(\frac{4 \cos k_i - \cos 2k_i}{3} \right)}{(\widetilde{k}^2)^2} \right] \equiv p^2 \mathcal{M}(k). \quad (\text{B27})$$

The equivalent expression in the continuum case is $p^2/3k^4$. Re-arranging the terms a little, we can write

$$\frac{C_2}{16\pi^2} = \frac{-1}{24} \int_{k, \mathfrak{R}^3 - \text{BZ}} \frac{1}{k^5} + \int_{k, \text{BZ}} \frac{1}{8k} \left(\mathcal{M}(k) - \frac{1}{3k^4} \right) + \int_{k, \text{BZ}} \mathcal{M}(k) \left[I_L(k) - \frac{1}{8k} - \frac{\xi}{4\pi} \right]. \quad (\text{B28})$$

We have seen the first integral. The second gives $.0310757695/16\pi^2$ and the last gives $.0142016/16\pi^2$; so $C_2 = .0334416$.

Next we must compute the $O(p^0)$ part of the setting sun diagram. The continuum diagram is IR and UV log divergent, while the lattice diagram is only IR log divergent. It is convenient to IR regulate both by introducing a mass on one line. In this case the continuum integral can be performed in $\overline{\text{MS}}$, leaving a lattice integral minus an analytically determined counterterm [20,21]. Choosing to separate the renormalization dependence along with the same finite constant as in the previous literature [20,21], the constant C_3 is given by

$$\frac{C_3}{(4\pi)^2} = \lim_{m \rightarrow 0} \left\{ \int_{k, \text{BZ}} \frac{1}{\widetilde{k}^2 + m^2} I_L(k) - \frac{1}{16\pi^2} \left[\frac{1}{2} + \ln \frac{6}{m} \right] \right\}. \quad (\text{B29})$$

The problem with this expression is the logarithm. To remove it, we add and subtract $I_C(k) = 1/8k$ to $I_L(k)$. The integral

$$\int_{k, \text{BZ}} \frac{1}{\widetilde{k}^2 + m^2} \left[I_L(k) - \frac{1}{8k} \right] \quad (\text{B30})$$

is IR convergent, and the $m \rightarrow 0$ limit may be taken immediately. It evaluates to $-.06858432/16\pi^2$, unless we use the unimproved lattice Laplacian, in which case it is $.60953343/16\pi^2$. We re-arrange the remaining terms to be

$$\int_{k, \text{BZ}} \left(\frac{1}{\widetilde{k}^2 + m^2} - \frac{1}{k^2 + m^2} \right) \frac{1}{8k} + \int_{k, \text{BZ}} \frac{1}{8k(k^2 + m^2)} - \frac{1}{16\pi^2} \left[\frac{1}{2} + \ln \frac{6}{m} \right]. \quad (\text{B31})$$

Again, for the first integral the $m \rightarrow 0$ limit may be taken immediately, and the numerical value is $.161799607/16\pi^2$, or $.43364112015/16\pi^2$ if we use the unimproved Laplacian. For the last integral, we cut the integration region into the ball of radius π and the region within the Brillouin zone but outside the ball:

$$\int_{k, \text{BZ}} \frac{1}{8k(k^2 + m^2)} = \frac{1}{2\pi^2} \int_0^\pi \frac{k^2 dk}{8k(k^2 + m^2)} + \int_{k, \text{BZ}} \frac{1}{8k(k^2 + m^2)} \Theta(|k| - \pi). \quad (\text{B32})$$

The first integral is easy and gives $\ln(\pi/m)/16\pi^2$ plus terms power suppressed in m . When added to $(-1/16\pi^2)(\ln(6/m) + 1/2)$, this cancels the $\ln(m)$, leaving $(1/16\pi^2)(\ln(\pi/6) - 1/2)$.

The final integral has had the small k part of the integration range removed, so the $m \rightarrow 0$ limit is trivial. It can then be reduced to

$$\frac{1}{16\pi^2} \int \frac{d\Omega}{4\pi} \ln(R(\text{cube}) - R(\text{ball})) = \frac{1}{16\pi^2} \frac{12}{\pi} \int_0^{\pi/4} d\phi \int_0^{\arctan(\sec \phi)} \sin(\theta) d\theta \ln(\sec(\theta)) \quad (\text{B33})$$

which numerically equals $.19233513195/16\pi^2$. Note that at no point have we had to deal numerically with an integral which is log divergent in m , or which still contains m at all.

Combining terms gives $C_3 = -.86147916$, unless we use the unimproved lattice Laplacian, in which case it is $C_{3,U} = .08848010$.

4. Three-loop result for $\delta\phi^2$

In principle, one could extend all the renormalization counterterms we have considered to three loop order. However, for many of them, this requires including mixing of different dimensions of operator insertions and including counterterms for radiatively induced high-dimension operators in the Lagrangian. However, the three-loop contribution to the additive counterterm $\delta\phi^2$ is an exception: it gives the $O(a)$ corrections to $\Delta\langle\phi^2\rangle_c$, and we've already seen that we can ignore higher-dimensional operators at this order. The calculation of $\delta\phi^2$ is the least complicated of the 3-loop calculations we might envision, and does not require the result of any other 3-loop calculations or any of the new counterterms which would be needed in a complete 3-loop matching. The relevant diagrams are given in Fig. 23. We find

$$\delta\phi_{3l}^2 - \delta\phi_{2l}^2 = \left[\left(\frac{N+2}{6} \right)^2 \xi^2 \Sigma + \frac{(N+2)}{18} (C_4 - 3\Sigma C_1 - \Sigma C_2 + \xi \log(a\bar{\mu})) \right] \frac{Nu^2}{(4\pi)^3} - \frac{\xi}{4\pi} Nr. \quad (\text{B34})$$

Here the new constant C_4 arises from the basketball diagram of Figure 23, together with part of the mass-squared counterterm diagram. The explicit renormalization scale dependence in (B34) cancels the implicit dependence of $r = r(\bar{\mu})$ in the last term.

Our definition of C_4 is that $(C_4 + \xi \log(a\mu))/(4\pi)^3$ equals the lattice value of the basketball diagram, (A) in Fig. 23, minus diagram (C) taking only the setting sun part of the two loop mass counterterm. Explicitly,

$$\frac{C_4 + \xi \log(a\mu)}{(4\pi)^3} = \int_{k,\text{BZ}} \frac{1}{(\tilde{k}^2)^2} \left(\int_{p,\text{BZ}} \frac{1}{\tilde{p}^2} [I_L(p+k) - I_L(p)] + \int_{p,\mathbb{R}^3} \frac{1}{p^2} I_C(p) \right)$$

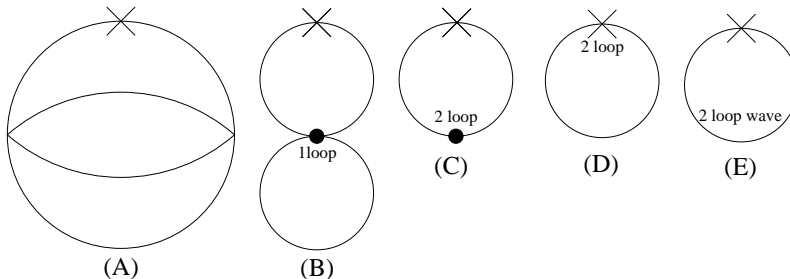


FIG. 23. Three-loop vacuum diagrams needed for $\delta\phi^2$ at 3 loops. There are 7 additional diagrams either involving 1 loop mass counterterms or tadpoles, which cancel among themselves.

$$- \int_{k, \mathbb{R}^3} \frac{1}{k^4} \int_{p, \mathbb{R}^3} \frac{1}{p^2} I_C(p+k). \quad (\text{B35})$$

Here $I_L(p+k)$ and $I_C(p+k)$ arise from the basketball diagram, while $I_L(p)$ and $I_C(p)$ are from the setting sun piece of the counterterm. Every term here is implicitly IR regulated by a common infinitesimal mass on every propagator, but the way we will perform the integrations means that we will never need this regulation explicitly. Also, continuum integrals are implicitly renormalized in $\overline{\text{MS}}$, which will be relevant.

It is convenient to add and subtract the appropriate factor to put the $I_C(p+k)$ factor inside the BZ k integral. We add and subtract

$$\left[\int_{k, \text{BZ}} \frac{1}{(\tilde{k}^2)^2} - \int_{k, \mathbb{R}^3} \frac{1}{k^4} \right] \int_{p, \mathbb{R}^3} \frac{1}{p^2} I_C(p+k). \quad (\text{B36})$$

The p integral can be evaluated in $\overline{\text{MS}}$, (note that we do not need its value in the deep IR where the implicit mass regularization becomes important), and gives

$$\int_{p, \mathbb{R}^3} \frac{1}{p^2} I_C(p+k) = \frac{1.5 - \log(k/\mu)}{16\pi^2}. \quad (\text{B37})$$

The constant terms can be pulled out of the k integrations; the remaining k integral is Eq. (B6) and gives $\xi/4\pi$. The constant parts therefore yield $(1.5 + \log(a\mu))\xi/(64\pi^3)$. The $\ln k$ leads to the integral

$$\frac{1}{16\pi^2} \left(\int_{k, \text{BZ}} \frac{-\ln(ak)}{(\tilde{k}^2)^2} - \int_{k, \mathbb{R}^3} \frac{-\ln(ak)}{k^4} \right) = \frac{0.30837}{64\pi^3} \quad (\text{B38})$$

for the improved Laplacian. Eq. (B35), after subtracting Eq. (B36), becomes

$$\int_{k, \text{BZ}} \frac{1}{(\tilde{k}^2)^2} \left(\int_{p, \text{BZ}} \frac{1}{\tilde{p}^2} [I_L(p+k) - I_L(p)] - \int_{p, \mathbb{R}^3} \frac{1}{p^2} [I_C(p+k) - I_C(p)] \right). \quad (\text{B39})$$

It is convenient to split off the part of the continuum p integration which lies outside the Brillouin zone as a separate integration, which does not suffer from divergences:

$$\frac{1}{8} \int_{k, \text{BZ}} \frac{1}{(\tilde{k}^2)^2} \int_{p, \mathbb{R}^3 - \text{BZ}} \left(\frac{1}{p^3} - \frac{1}{p^2|p+k|} \right) = \frac{.00031757}{64\pi^3}. \quad (\text{B40})$$

This leaves as the final integral we must consider,

$$\int_{k, \text{BZ}} \frac{1}{(\tilde{k}^2)^2} \int_{p, \text{BZ}} \left(\frac{1}{\tilde{p}^2} [I_L(p+k) - I_L(p)] - \frac{1}{p^2} [I_C(p+k) - I_C(p)] \right). \quad (\text{B41})$$

This integration is finite and over a finite integration region (provided we make a prescription that the argument of the p integral is interpreted as the average over p and $-p$ of the quantity written). The integration is nine dimensional and contains some delicate integrable singularities. We find it convenient to use adaptive Monte Carlo integration rather than quadratures. Monte Carlo integration is somewhat problematical when there are integrable singularities. Rather than finding clever changes of variables to get rid of such singularities, the simplest thing to do is to include a small mass in all the propagators (thus cutting off all singularities), vary that mass, and then numerically extrapolate the zero mass limit from the results of the Monte Carlo integrations. Our result for the integral (B41) is $(0.0985 \pm 0.006)/(4\pi)^3$. Combining terms, we then have $C_4 = 0.2817(6)$ for the improved Laplacian.

5. Minimalist expression for $\Delta\langle\phi^2\rangle_c$ through $O(a)$

Some of the development in the preceding sections is unnecessary for the isolated goal of getting an $O(a)$ improvement of $\Delta\langle\phi^2\rangle$. It is possible to combine the previous results in the more compact form

$$\Delta\langle\phi^2\rangle_{\text{cont}} = \frac{Z_m}{Z_\phi} \Delta\langle\Phi^2\rangle_{\text{lat}} + \frac{\xi}{4\pi} ar_1 - \frac{(N+2)}{18} \frac{\mathcal{C}}{(4\pi)^3} au_0^2 + O(u^3), \quad (\text{B42a})$$

$$\mathcal{C} \equiv C_4 + \xi \ln 6 + \xi C_3. \quad (\text{B42b})$$

Here Φ is the *bare* lattice field, and u_0 the bare lattice coupling, corresponding to the bare lattice action (2.1);

$$\Delta\langle\Phi^2\rangle_{\text{lat}} = \langle\Phi^2\rangle_{\text{lat}} - \frac{\Sigma}{4\pi a}; \quad (\text{B42c})$$

r_1 stands for the tadpole-adjusted mass,

$$r_1 \equiv r_0 + \left(\frac{N+2}{6}\right) \frac{\Sigma}{4\pi a} u_0, \quad (\text{B42d})$$

which is $O(u^2)$ near the transition; and r_0 is the bare mass used in the bare lattice action (2.1). We have retreated from lattice units and explicitly show all factors of a . Since $\Delta\langle\Phi^2\rangle$ is $O(u)$ near the transition, we only need the one-loop result

$$\frac{Z_m}{Z_\phi} \simeq 1 + \frac{(N+2)}{6} u \frac{\xi}{4\pi} \quad (\text{B42e})$$

for Z_m/Z_ϕ .

To finish the relationship between the measurement of $\Delta\langle\phi^2\rangle/u$ and the bare fields and parameters of the lattice Lagrangian, we only need the one-loop relationship between the continuum and bare lattice couplings:

$$u_0 \simeq u + \frac{(N+8)}{6} u^2 \frac{\xi}{4\pi}. \quad (\text{B42f})$$

The form (B42) has the conceptual advantage of not introducing the renormalization scale $\bar{\mu}$, since its introduction is unnecessary if one's only interest is in $\Delta\langle\phi^2\rangle_c$ and not the value of r_c . Eq. (B42) also makes clear that nothing depends on C_1 and C_2 at this order, so that one doesn't really need those integrals. And it makes clearer that there is no $O(a^0)$ correction to $\Delta\langle\phi^2\rangle$, which is obscured by eqs. (2.15) and (2.16). That is,

$$\Delta\langle\phi^2\rangle_{\text{cont}} = \Delta\langle\Phi^2\rangle_{\text{lat}} + O(au^2), \quad (\text{B43})$$

as in (2.11).

However, this is not how we have implemented our calculation of $\Delta\langle\phi^2\rangle_c$ when quoting numbers from simulations. What we have done is described in the text and the earlier parts of this appendix and, though equivalent through $O(a)$, will give slightly different numerical values because of differences in higher orders in a .

APPENDIX C: LOGS IN LARGE VOLUME SCALING FOR $\alpha = 0$

In this section, we review standard renormalization group arguments about the free energy and verify that a $t^2 \ln L$ term appears in the free energy when $\alpha = 0$. If one increases renormalization scale by a “blocking” factor of b , the free energy density of the blocked system is related to the free energy of the original system by a transformation law of the form

$$\mathcal{F}(\{K\}) = \mathcal{G}(\{K\}) + b^{-d}\mathcal{F}(\{K'\}), \quad (\text{C1})$$

where \mathcal{F} is the free energy per block, $\{K\}$ represents the couplings of the theory, and \mathcal{G} is an analytic function (depending on b) that represents the contributions to the free energy from the degrees of freedom that have been blocked.⁹ Iterating n times, this becomes

$$\mathcal{F}(\{K\}) = \sum_{j=0}^{n-1} b^{-jd}\mathcal{G}(\{K^{(j)}\}) + b^{-nd}\mathcal{F}(\{K^{(n)}\}), \quad (\text{C2})$$

where $\{K^{(j)}\}$ is the j th iterate of $\{K\}$. If we start with a block size of a and iterate all the way out to size L , we have $n = \log_b(L/a)$.

For t very small but non-zero, the description of the system will first flow towards the critical point, as one blocks to larger and larger distances. But it will then eventually flow away from the fixed point, closely following one of the two unique “outflow” trajectories from the fixed point (one for $t > 0$ and one for $t < 0$), corresponding to all irrelevant couplings being set to zero. The inhomogeneous part \mathcal{G} of the transformation law (C2) will generate singular behavior as $t \rightarrow 0$, which may then be written as

$$\mathcal{F}(t) \sim \sum_{j=0}^{\log_b(L/a)} b^{-jd}\mathcal{G}(b^{jy_t}t), \quad (\text{C3})$$

where $b^{jy_t}t$ parameterizes flow along the outflow trajectory. For the infrared behavior at large L and small t , we can replace the sum by an integration. Changing integration variable to $s \equiv b^{jy_t}t$,

$$\mathcal{F}(t) \sim \frac{t^{d/y_t}}{y_t \ln b} \int_t^{t(L/a)^{y_t}} s^{\alpha-3}\mathcal{G}(s) ds, \quad (\text{C4})$$

where $\alpha = 2 - d/y_t$. For $\alpha = 0$, this is

$$\mathcal{F}(t) \sim \frac{2t^2}{d \ln b} \int_t^{t(L/a)^{d/2}} s^{-3}\mathcal{G}(s) ds. \quad (\text{C5})$$

To help tame the singularity as $s \rightarrow 0$, integrate by parts two times. This leaves an integral proportional to

⁹ Our presentation follows, for example, chapter 3 of Ref. [22], which is one of many nice introductions to the renormalization group. Our \mathcal{F} and \mathcal{G} are that reference’s f and g . We use \mathcal{F} to avoid confusion with f in the text, which was the free energy per physical volume rather than per block.

$$t^2 \int_t^{t(L/a)^{d/2}} s^{-1} \mathcal{G}''(s) ds \quad (\text{C6})$$

plus terms which fit the too-naive scaling form (4.12). The remaining integral can be rewritten as

$$\mathcal{G}''(0) t^2 \ln(L^{-d/2}) + t^2 \int_t^{t(L/a)^{d/2}} s^{-1} [\mathcal{G}''(s) - \mathcal{G}''(0)] ds. \quad (\text{C7})$$

The second term has the desired analyticity properties of the too-naive scaling form (4.12), and the first term is the logarithm of Privman and Rudman appearing in (4.14).

APPENDIX D: LARGE VOLUME SCALING OF CUMULANT INTERSECTIONS

First, let's quickly reproduce Binder's result (3.5) for the scaling of $r_\times(L_1, L_2) - r_c$. For large L , we will focus on the scaling piece of the cumulant which, in the notation of section IV A, is

$$C(t, \{u_j\}, L^{-1}) \sim C_{\text{sing}}(b^{y_t} t, \{u_j b^{y_j}\}, b/L). \quad (\text{D1})$$

Choosing $b = L$,

$$C \simeq C_{\text{sing}}(L^{y_t} t, \{u_j L^{y_j}\}, 1), \quad (\text{D2})$$

where C_{sing} is a universal scaling function. Now treat $L^{y_t} t$ and $u_j L^{y_j}$ as small and Taylor expand, keeping track of only the most important irrelevant operator u_j ,

$$C \simeq C_{\text{sing}}(0, 0, 1) + AL^{y_t} t + BL^{-\omega}. \quad (\text{D3})$$

Note that A and $C_{\text{sing}}(0, 0, 1)$ are universal, but B is not, because it depends on the value of u_j . Now look for the intersection for two different system sizes:

$$C_{\text{sing}}(0, 0, 1) + AL_1^{y_t} t + BL_1^{-\omega} = C_{\text{sing}}(0, 0, 1) + AL_2^{y_t} t + BL_2^{-\omega}, \quad (\text{D4})$$

which has solution

$$t \simeq \frac{B(L_1^{-\omega} - L_2^{-\omega})}{A(L_2^{y_t} - L_1^{y_t})} \quad (\text{D5})$$

up to corrections suppressed by additional powers of $1/L$. This is just the scaling (3.5) quoted for $r_\times - r_c$. (And one sees *a posteriori* that it was justified to treat $L^{y_t} t$ as small in the $L \rightarrow \infty$ limit.) All that is necessary to derive the scaling (3.6) of C_\times is to plug (D5) back into (D4) and rename $C_{\text{sing}}(0, 0, 1)$ as C_c .

In the main text, our procedure for defining the nominal transition in finite volume, for our small ua simulations, is to find the point where $C = C_c$. From (D4), one may verify that this prescription gives

$$t \simeq \frac{B}{A} L^{-y_t - \omega} \sim L^{-y_t - \omega}, \quad (\text{D6})$$

as asserted in the main text.

APPENDIX E: SMALL Lu EXPANSION OF $\Delta\langle\phi^2\rangle_c$

In this appendix, we compute the expected result for $\Delta\langle\phi^2\rangle_c$ for small volumes in the continuum limit, where we define the nominal critical temperature in such volumes using Binder cumulants, as explained in Sec. III. We have repeatedly described “short distance” physics (distance small compared to $1/u$) as perturbative, and so for small volumes ($L \ll 1/u$), one might first try simple perturbation theory to compute $\Delta\langle\phi^2\rangle$. The leading-order diagram contributing to $\Delta\langle\phi^2\rangle$ is shown in Fig. 20d and corresponds to

$$\langle\phi^2\rangle \simeq \frac{N}{L^3} \sum_{\mathbf{p}} \frac{1}{p^2 + r}, \quad (\text{E1})$$

where for the sake of generality we have considered an $O(N)$ model, and the actual case of interest is $N = 2$. The sum is over the discrete momenta $\mathbf{p} = 2\pi\mathbf{n}/L$ associated with the $L \times L \times L$ periodic volume. There is a problem with (E1), however. Consider the mean-field theory approximation $r_c = 0$ to the critical value of r . The sum then has a infrared divergent term associated with $\mathbf{p} = 0$. The problem is that it is more accurately large momentum physics which is perturbative, rather than small distance physics. So, even when $L \rightarrow 0$, the physics associated with the $\mathbf{p} = 0$ modes is non-perturbative. Since this is only one mode, we simply analyze it separately, and then treat all the $\mathbf{p} \neq 0$ modes perturbatively.

1. The case $r = 0$: leading order

To illustrate the calculation, let us first compute $\Delta\langle\phi^2\rangle$ if $r = 0$. We’ll later come back to consider the actual r that is chosen by the criteria of our simulations that the cumulant $C = C_c$. Consider the approximation S_0 to the action where we ignore everything but the $\mathbf{p}=0$ modes ϕ_0 :

$$S_0 = \int d^3x \left[|\nabla\phi_0|^2 + \frac{u}{4!} |\phi_0|^4 \right] = \frac{L^3 u}{4!} |\phi_0|^4. \quad (\text{E2})$$

Note that this result holds on the lattice as well as in the continuum. The $\mathbf{p} = 0$ contribution to $\Delta\langle\phi^2\rangle$ is then

$$\langle\phi_0^2\rangle \simeq \frac{\int d^N\phi_0 e^{-S_0} |\phi_0|^2}{\int d^N\phi_0 e^{-S_0}} = \left(\frac{4!}{L^3 u} \right)^{1/2} \frac{\int d^N x e^{-x^4} x^2}{\int d^N x e^{-x^4}} = \left(\frac{4!}{L^3 u} \right)^{1/2} \frac{\Gamma\left(\frac{N+2}{4}\right)}{\Gamma\left(\frac{N}{2}\right)}. \quad (\text{E3})$$

By dimensional analysis, the leading perturbative contribution of the $\mathbf{p} \neq 0$ modes to $\langle\phi^2\rangle$ should be order L^{-1} and so is dominated by the zero-mode contribution (E3). Specializing to $N = 2$, we then have

$$\frac{\langle\phi^2\rangle_{r=0}}{u} = \frac{\sqrt{4!}}{(Lu)^{3/2}} + O((Lu)^{-1}) \simeq \frac{2.76395}{(Lu)^{3/2}} + O((Lu)^{-1}). \quad (\text{E4})$$

As we’ll see explicitly below, the UV subtraction that converts $\langle\phi^2\rangle$ to $\Delta\langle\phi^2\rangle$ in the continuum limit is not relevant until next order in $(Lu)^{-1}$, and so $\Delta\langle\phi^2\rangle/u$ also has the expansion (E4).

2. The case $r = 0$: next-to-leading order

Now consider the leading-order perturbative contribution $\delta\langle\phi^2\rangle$ of the non-zero modes to $\langle\phi^2\rangle$ from (E1):

$$\delta\langle\phi^2\rangle \simeq \frac{N}{L^3} \sum_{\mathbf{p}\neq 0} \frac{1}{p^2}. \quad (\text{E5})$$

This sum is UV divergent, and the UV divergence is simply the free-field divergence discussed in section (II A). It is subtracted when we compute $\Delta\langle\phi^2\rangle$ as opposed to $\langle\phi^2\rangle$. Note that our prescriptions (2.11) or (2.15) for computing $\Delta\langle\phi^2\rangle$ in our simulations involve subtracting the *infinite volume* free-field result for $\langle\phi^2\rangle$. In the continuum limit, this subtraction turns the perturbation (E5) into

$$\delta\Delta\langle\phi^2\rangle = \frac{N}{L^3} \sum_{\mathbf{p}\neq 0} \frac{1}{p^2} - N \int_{\mathbf{p}} \frac{1}{p^2} = \frac{N}{(2\pi)^2 L} \left[\sum_{\mathbf{n}\neq 0} \frac{1}{n^2} - \int \frac{d^3 n}{n^2} \right]. \quad (\text{E6})$$

Individually, the sums and integrals above must be consistently regulated, for example by dimensional regularization or by keeping the system on a lattice with arbitrarily small lattice spacing.

There are a number of ways to evaluate the result numerically. One is to start by regulating with dimensional regularization, working in d spatial dimensions. Then

$$\delta\Delta\langle\phi^2\rangle = \frac{N}{L^d} \sum_{\mathbf{p}\neq 0} \frac{1}{p^2} - N \int_{\mathbf{p}} \frac{1}{p^2} = \frac{N}{(2\pi)^2 L^{d-2}} \left[\sum_{\mathbf{n}\neq 0} \frac{1}{n^2} - \int \frac{d^d n}{n^2} \right]. \quad (\text{E7})$$

Now rewrite

$$\frac{1}{n^2} = \int_0^\infty ds e^{-sn^2}. \quad (\text{E8})$$

The n_1, n_2, \dots sums and integrals then factor, giving

$$\sum_{\mathbf{n}\neq 0} \frac{1}{n^2} - \int \frac{d^d n}{n^2} = \int_0^\infty ds \left\{ [\theta_3(e^{-s})]^d - 1 - \left(\frac{\pi}{s}\right)^{d/2} \right\}, \quad (\text{E9})$$

where

$$\theta_3(q) \equiv \sum_{k=-\infty}^{\infty} q^{-(k^2)} \quad (\text{E10})$$

is a special case of an elliptic theta function. The integral on the right-hand side of (E9) is absolutely convergent in $d = 3$, so we can now dispense with dimensional regularization and set d to three. The integral is then easily done numerically, giving

$$\sum_{\mathbf{n}\neq 0} \frac{1}{n^2} - \int \frac{d^d n}{n^2} \simeq -8.91363. \quad (\text{E11})$$

For $N = 2$, one then has

$$\frac{\delta\Delta\langle\phi^2\rangle_{r=0}}{u} \simeq -\frac{0.451570}{Lu}. \quad (\text{E12})$$

The effect of interactions in the non-zero mode sector will be perturbative for small Lu and will give higher order contributions to $\Delta\langle\phi^2\rangle$. However, we must also consider interactions of the zero mode ϕ_0 with the non-zero modes, which will give corrections to the action S_0 used in our earlier analysis of ϕ_0 . For instance, the coupling u in S_0 will pick up corrections of order Lu^2 . This will generate an $O(Lu)$ relative correction to the zero-mode contribution (E4), and so that correction will be higher order than the contribution (E12) computed above. A similar story will hold for corrections to r (and for the effects of higher-dimensional interactions) with the complication that r will receive some infinite contributions in the continuum limit, corresponding to the usual mass renormalization. The latter is absorbed by the usual renormalization of r , and so one has

$$\frac{\delta\langle\phi^2\rangle_{r=0}}{u} \simeq \frac{2.76395}{(Lu)^{3/2}} - \frac{0.451570}{Lu} + O((Lu)^{-1/2}) \quad (\text{E13})$$

if one interprets the r in the condition $r = 0$ as being renormalized r . (The details of the renormalization scheme will not matter at the order shown.)

3. The case $C = C_c$

Now, instead of setting $r = 0$, we will choose r so that the cumulant C is equal to its critical value. Let's begin with a leading-order analysis and so focus on just the $\mathbf{p} = 0$ sector. For general r , we then have

$$S_0 = \frac{L^3 r}{2} |\phi_0|^2 + \frac{L^3 u}{4!} |\phi_0|^4 \quad (\text{E14})$$

and

$$\langle\phi_0^{2k}\rangle = \frac{\int d^N \phi_0 e^{-S_0} |\phi_0|^{2k}}{\int d^N \phi_0 e^{-S_0}}. \quad (\text{E15})$$

By a change of variables, this can be rewritten as

$$\langle\phi_0^{2k}\rangle = \left(\frac{4!}{L^3 u}\right)^{k/2} \frac{I_k(R)}{I_0(R)} \quad (\text{E16})$$

where

$$I_k(R) \equiv \int_0^\infty dy e^{-y^2 - R y} y^{k+(N-2)/2}, \quad (\text{E17})$$

and

$$R \equiv \frac{r}{2} \left(\frac{4!}{L^3 u}\right)^{1/2}. \quad (\text{E18})$$

Now note that the volume average $\bar{\phi}$ of the field, used in the definition of the cumulant, is simply ϕ_0 . Specializing now to $N = 2$ and doing the I_k integrals, one obtains

$$I_0(R) = \frac{\sqrt{\pi}}{2} e^{R^2/4} \operatorname{erfc}\left(\frac{R}{2}\right), \quad (\text{E19})$$

$$I_1(R) = \frac{1}{2}[1 - R I_0(R)], \quad (\text{E20})$$

$$I_2(R) = \frac{1}{4}[-R + (R^2 + 2)I_0(R)]. \quad (\text{E21})$$

The cumulant can be written

$$C \equiv \frac{\langle \phi_0 \rangle^4}{\langle \phi_0^2 \rangle^2} \simeq \frac{I_2(R) I_0(R)}{[I_1(R)]^2}. \quad (\text{E22})$$

A numerical search for the point where $C = C_c \simeq 1.234$ gives

$$R \simeq -2.59093. \quad (\text{E23})$$

At this R , the zero-mode contribution to $\langle \phi^2 \rangle$ is then

$$\langle \phi^2 \rangle_c = \left(\frac{4!}{L^3 u} \right)^{1/2} \frac{I_1(R)}{I_0(R)} + O((Lu)^{-1}) = \frac{6.61341}{(L^3 u)^{1/2}} + O((Lu)^{-1}). \quad (\text{E24})$$

Since the result for R is a pure number, the definition (E18) of R shows that r is of order $(L^3 u)^{-1/2}$, which is smaller by a power of $(Lu)^{-1/2}$ than any of the non-zero momenta, which are order L^{-1} . So r can be ignored in finding the leading contribution of the non-zero modes, with the effect that $\delta\Delta\langle \phi^2 \rangle$ is the same as in the earlier $r = 0$ analysis. Adding (E24) and (E12) then produces the result (4.15) quoted in the main text.

APPENDIX F: SYSTEM SIZE AND THE SIMULATIONS OF GRÜTER *et al.*

One of the applications of O(2) field theory is to studying the corrections to the critical temperature, due to interactions, for Bose-Einstein condensation of a nearly-ideal non-relativistic Bose gas. This application has been previously studied using numerical techniques. Our discussion of system size in section IV C has implications for an early study by Grüter *et al.* [18], which is that much of the data collected was likely in insufficiently large volume. These simulations did not make use of O(2) field theory: They worked in the canonical ensemble and studied the path integral for a fixed number N_p of particles in a finite volume V . If no attempt were made to fit for large volume corrections, then Fig. 4 makes it clear that one should take roughly $Lu \geq 400$ to keep those corrections moderately small. We can translate this condition on system size to the context of Bose-Einstein condensation by translating the parameter u of the O(2) field theory. For this application, the relation is [2] $u = 96\pi^2 a/\lambda^2$, where a is the scattering length of the atoms, $\lambda = \hbar\sqrt{2\pi/mk_B T}$ is the thermal wavelength, and m is the mass of the atoms. Using the ideal gas approximation $T_c \simeq T_0 = (2\pi\hbar^2/k_B m)[n/\zeta(\frac{3}{2})]^{2/3}$ for the critical temperature, one can write

$$na^3 \simeq \left(\frac{Lu}{96\pi^2} \right)^3 \frac{\zeta(\frac{3}{2})^2}{N_p} \quad (\text{F1})$$

at the transition. The condition $Lu \geq 400$ may then be translated into the condition

$$na^3 \geq \frac{0.51}{N_p}. \quad (\text{F2})$$

The largest N_p used in the simulations of Grüter *et al.* was $N_p = 216$, and their extraction of the critical temperature depended on results with $N_p = 125$ as well. For the latter, our rough condition for being in large enough volume then requires $na^3 \geq 0.004$. This makes suspect (a) their small na^3 results, which go down to $na^3 = 10^{-5}$, and (b) their extrapolation of the corrections to the ideal gas result for the critical temperature in the $na^3 \rightarrow 0$ limit. (See Fig. 3 of Ref. [18].)

REFERENCES

- [1] P. Arnold and G. Moore, cond-mat/0103228.
- [2] G. Baym, J.-P. Blaizot, M. Holzmann, F. Laloë, and D. Vautherin, Phys. Rev. Lett. **83**, 1703 (1999).
- [3] D. Bedingham and T. Evans, hep-ph/0011286.
- [4] P. Arnold and S. Tkachenko, in preparation.
- [5] P. Arnold and B. Tomášik, in preparation.
- [6] G. Watson, Quart. J. Math. (Oxford, 1st series) **10**, 266 (1939).
- [7] J. Goodman and A. D. Sokal, Phys. Rev. Lett. **56**, 1015 (1986); J. Goodman and A. D. Sokal, Phys. Rev. D **40**, 2035 (1989).
- [8] K. Binder, Phys. Rev. Lett. **47**, 693 (1981); Z. Phys. B **43**, 119 (1981).
- [9] M. Hasenbusch and T. Török, J. Phys. A: Math. Gen. **32**, 6361 (1999).
- [10] M. Fisher, Phys. Rev. **176**, 257 (1968).
- [11] M.N. Barber in *Phase Transitions and Critical Phenomena*, vol. 8, eds. C. Domb and J.L. Lebowitz (New York: Academic Press, 1983).
- [12] V. Privman and M.E. Fisher, Phys. Rev. **B30**, 322 (1984).
- [13] J.A. Lipa, D.R. Swanson, J.A. Nissen, T.C.P. Chui, and U.E. Israelsson, Phys. Rev. Lett. **76**, 944 (1996).
- [14] R. Guida and J. Zinn-Justin, J. Phys. A: Math. Gen. **31**, 8103 (1998).
- [15] V. Privman and J. Rudnick, J. Phys. A: Math. Gen. **19**, L1215 (1986).
- [16] G. Baym, J.-P. Blaizot, and J. Zinn-Justin, Europhys. Lett. **49**, 150 (2000).
- [17] P. Arnold and B. Tomášik, Phys. Rev. **A62**, 063604 (2000).
- [18] P. Grüter, D. Ceperley, and F. Laloë, Phys. Rev. Lett. **79**, 3549 (1997).
- [19] G. D. Moore, Nucl. Phys. B **493**, 439 (1997) [hep-lat/9610013]; G. D. Moore, Nucl. Phys. B **523**, 569 (1998) [hep-lat/9709053].
- [20] K. Farakos, K. Kajantie, K. Rummukainen and M. Shaposhnikov, Nucl. Phys. B **442**, 317 (1995) [hep-lat/9412091].
- [21] M. Laine and A. Rajantie, Nucl. Phys. B **513**, 471 (1998) [hep-lat/9705003].
- [22] J. Cardy, *Scaling and Renormalization in Statistical Physics* (Cambridge University Press: Cambridge, 1997).